2007-03-30

The Role of Phosducin-like Protein as a Co-chaperone with the Cytosolic Chaperonin Complex in Assembly of the G Protein βγ Subunit Dimer

Paul Jayson Ludtke
Brigham Young University - Provo

THE ROLE OF PHOSDUCIN-LIKE PROTEIN AS A CO-CHAPERONE WITH THE CYTOSOLIC CHAPERONIN COMPLEX IN THE ASSEMBLY OF THE G PROTEIN βγ SUBUNIT DIMER

by

Paul Ludtke

A thesis submitted to the faculty of

Brigham Young University

in partial fulfillment of the requirements for the degree of

Master of Science

Department of Chemistry and Biochemistry

Brigham Young University

April, 2007

BRIGHAM YOUNG UNIVERSITY

GRADUATE COMMITTEE APPROVAL

of a thesis submitted by

Paul Ludtke

This thesis has been read by each member of the following graduate committee and by majority vote has been found to be satisfactory

_____	_____
Date	Dr. Barry M. Willardson, Chair
_____	_____
Date	Dr. David M. Belnap
_____	_____
Date	Dr. Allen T. Buskirk
_____	_____
Date	Dr. David Busath

BRIGHAM YOUNG UNIVERSITY

As chair of the candidate's graduate committee, I have read the thesis of Paul Ludtke in its final form and have found that (1) its format, citations, and bibliographical style are consistent and acceptable and fulfill university and department style requirements; (2) its illustrative materials including figures, tables, and charts are in place; and (3) the final manuscript is satisfactory to the graduate committee and is ready for submission to the university library.

_____ _____

Date Dr. Barry M. Willardson
Chair, Graduate Committee

Accepted by the department

_____

David V. Dearden
Graduate Coordinator

Accepted for the College

_____

Thomas W. Sederberg
Associate Dean
College of Physical and Mathematical Sciences

TABLE OF CONTENTS

LIST OF FIGURES

ABBREVIATIONS

ATP	adenosine tri-phosphate
C-	carboxy-terminus
CCT	cytosolic chaperonin tailless containing TCP-1
CHO	chinese hamster ovary
CID	collision induced dissociation
CK2	casein kinase II
-EM	electron microscopy
G protein	guanine nucleotide binding protein
Gα	G protein alpha subunit
$G_t\alpha$	transducin (photoreceptor-specific G protein)
Gβ	G protein beta subunit
Gγ	G protein gamma subunit
Gβγ	G protein beta and gamma subunit dimer
GDP	guanosine diphosphate
GTP	guanosine triphosphate
HEK	human embryonic kidney
His	histadine
HPC4	human protein-C clone 4
N-	amino-terminus
PAGE	polyacrylamide gel electrophoresis
PCR	polmerase chain reaction
Pdc	phosducin
PFD	prefoldin
PhLP	phosducin-like protein
Q-ToF	quadrapole-time of flight
RRL	rabbit reticulocyte lysate
S/A	serine to alanine substitution
SDS	sodium dodecyl sulphate
Ser-	serine
TCP-1	tailless complex polypeptide-1
TEV	tobacco etch virus

ACKNOWLEDGEMETS

I would like to express my gratitude to Dr. Willardson for his example, teaching, and patience during this work. I would also like to express my appreciation to previous and present members of the Willardson lab; I have never worked with a finer group of people. Special thanks to contributions made by the group of Jose Valpuesta at the University of Madrid in Spain who provided the cryoelectron microscopy data. Finally, I would like to thank my graduate committee, the Department of Chemistry and Biochemistry and Brigham Young University for providing a quality environment for learning.

ABSTRACT

THE ROLE OF PHOSDUCIN-LIKE PROTEIN AS A CO-CHAPERONE WITH THE CYTOSOLIC CHAPERONIN COMPLEX IN THE ASEMBLY OF THE G PROTEIN βγ SUBUNIT DIMER

Phosducin-like protein (PhLP) has been shown to interact with the cytosolic chaperonin containing TCP-1 (CCT), and the βγ subunit dimer of heterotrimeric G proteins (Gβγ). Here we provide details obtained from cryo-electron microscopic and biochemical studies on the structure of the complex between the cytosolic chaperonin CCT and PhLP. Binding of PhLP to CCT occurs through only one of the two chaperonin rings, making multiple contacts with CCT through both its N- and C-terminal domains. In addition, we show that PhLP acts as a co-chaperonin along with CCT in mediating the assembly of the G protein βγ subunit and that assembly is dependant upon the phosphorylation of PhLP by the protein kinase CK2. Variants of PhLP lacking the CK2 phosphorylation sites, or variants with an inability to bind Gβγ block the assembly process and inhibit G protein signaling. PhLP forms a complex with CCT and nascent Gβ prior to the release of Gβγ from the ternary complex and subsequent association with the Gγ subunit to form the Gβγ dimer. In order to understand the mechanism of Gβγ dimer assembly and the role of PhLP phosphorylation in the assembly process, we provide here a method for the purification of the PhLP·CCT·Gβ ternary complex of sufficient purity for structural studies.

CHAPTER 1

THE POTENTIAL ROLE OF PHOSDUCIN-LIKE PROTEIN AND THE CYTOSOLIC CHAPERONIN COMPLEX IN G PROTEIN-MEDIATED SIGNAL TRANSDUCTION.

Eukaryotic cells employ heterotrimeric G proteins to transduce a wide variety of hormonal, neuronal, and sensory signals that control numerous physiological processes. As a result, malfunctions in G protein pathways contribute to many diseases (Rockman, Koch et al. 2002; Simonds 2003; Gainetdinov, Premont et al. 2004), and therapeutic agents targeting G protein-coupled receptors represent the single largest class of current pharmaceuticals (Schoneberg, Schulz et al. 2004). There are three fundamental steps in the propagation of a G protein-mediated signal. First, a ligand binds a receptor, resulting in a change in the packing of the seven transmembrane α-helices found in all G protein-coupled receptors. Second, the activated receptor catalyzes exchange of GDP for GTP on the α subunit of a heterotrimeric G protein (Gα) on the intracellular surface of the receptor. GTP binding causes Gα to dissociate from the G protein βγ subunit complex (Gβγ). Third, the Gα·GTP and Gβγ complexes control the activity of effector enzymes and ion channels that regulate the intracellular concentration of second messengers (cyclic nucleotides, inositol phosphates, and Ca^{2+}) and the plasma membrane electrical potential (mainly via K^+ channels). Changes in these properties in turn orchestrate the cellular response to the stimulus (Cabrera-Vera, Vanhauwe et al. 2003).

Phosducin-like protein (PhLP) is a member of the phosducin gene family (Miles, Barhite et al. 1993; Flanary, DiBello et al. 2000; Blaauw, Knol et al. 2003) that is believed to participate in G protein signaling by virtue of its ability to bind the Gβγ dimer with high affinity (Schroder and Lohse 1996; Thibault, Sganga et al. 1997; Savage, McLaughlin et al. 2000). Many *in vitro* and over-expression experiments have shown that PhLP binding to Gβγ blocks its ability to interact with Gα or effectors (Schroder and Lohse 1996; Thibault, Sganga et al. 1997; Gensse, Vitale et al. 2000; McLaughlin, Thulin et al. 2002; Humrich, Bermel et al. 2003). From these experiments, it was suggested that the physiological role of PhLP was to down-regulate G protein signaling by sequestering Gβγ. However, the results of several recent studies have seriously challenged this model. Specifically, disruption of the *PhLP1* gene in the chestnut blight fungus *cryphonectria parasitica* (Kasahara, Wang et al. 2000) and in the soil amoeba *Dictyostelium discoideum* (Blaauw, Knol et al. 2003) yielded the same phenotype as the disruption of the Gβ gene. Moreover, PhLP deletion blocked G protein signaling in *Dictyostelium* (Blaauw, Knol et al. 2003). In another study, the duration of opiate desensitization was prolonged in mice in which PhLP expression in the brain was inhibited by antisense oligonucleotide treatment (Garzon, Rodriguez-Diaz et al. 2002). All of these observations are the exact opposite of what would be predicted by the Gβγ sequestration model.

Further insight into the role of PhLP emerged as studies began to characterize the interaction of PhLP with a previously unidentified binding partner, the chaperonin containing tailless complex polypeptide 1 (CCT), a cytosolic molecular chaperone (McLaughlin, Thulin et al. 2002). Molecular chaperones are a large class of proteins that assist other proteins in attaining their active conformation. Among them, chaperonins are

a ubiquitous family of chaperones that have a common toroidal structure formed by the oligomerization of eight different 60-kDa subunits. The toroid is made of two rings placed back-to-back with each ring enclosing a cavity where folding occurs (Ellis, R.J. 1996). Chaperonins have been classically divided in two groups depending on whether they are found in eubacteria and in the endosymbiotic organelles (group I) (Ellis and Hartl 1999) or in archaea and the cytosol of eukarya (group II) (Gutsche, Essen et al. 1999). The monomers of every chaperonin known share a very similar three-domain structure (Braig, Otwinowski et al. 1994; Ditzel, Lowe et al. 1998): an equatorial domain that contains the nucleotide binding site and most of the interaction sites between the subunits of the same ring and of the opposite ring; an apical domain where the substrate binding site is located; and an intermediate domain that transmits to the apical domain the signals generated in the equatorial domain upon nucleotide binding. Chaperonins act on unfolded substrates by using a general mechanism that involves the recognition of the unfolded polypeptide by hydrophobic residues at the entrance of the chaperonin cavity, followed by folding of the polypeptide upon closure of the cavity induced by the binding of ATP and a co-chaperonin (Gomez-Puertas, Martin-Benito et al. 2004).

A more specific mechanism seems to operate for the group II eukaryotic cytosolic chaperonin CCT (chaperonin containing TCP-1), whose toroidal structure is made up of two rings composed of eight different but homologous proteins (Willison, K.R. 1999). The work carried out with the major CCT substrates, actin and tubulin, has shown that the recognition mechanism operates through defined CCT subunits and specific domains of the substrates, which have already acquired a large degree of native-like conformation before interacting with CCT. The conformational changes undergone by CCT upon

nucleotide binding would be used to actively fold the two cytoskeletal proteins (Gomez-Puertas, Martin-Benito et al. 2004) or to generate a structure apt to form a stable complex with other proteins (Valpuesta, J.M. 2004). In addition to its involvement in actin and tubulin folding, various other substrates have been characterized, including many WD40 repeat, 7-bladed β-propeller proteins. Among these various substrates, PhLP and more recently, the G protein β subunit have been shown to bind CCT (Lukov, Hu et al. 2005; Wells, Dingus et al. 2006). The focus of this thesis is to gain a better understanding of the functional consequences of the interactions of PhLP with its binding partners CCT, Gβγ, and the Gβ subunit.

CHAPTER 2

STRUCTURE OF THE COMPLEX BETWEEN THE CYTOSOLIC CHAPERONIN CCT AND PHOSDUCIN-LIKE PROTEIN.

Introduction–The interaction between PhLP and CCT appears to play a different role than that of a protein substrate being folded by a chaperonin. PhLP and its homologue Pdc are involved in the regulation of cell signaling through their interaction with the Gβγ. Binding of PhLP or Pdc prevents Gβγ from interacting with the Gα subunit or downstream effectors (Bauer, Muller et al. 1992; Lee, Ting et al. 1992; Hawes, Touhara et al. 1994; Gaudet, Bohm et al. 1996; McLaughlin, Thulin et al. 2002). Unlike protein folding substrates, PhLP has been shown to interact with CCT in its native form and to inhibit its actin folding activity (McLaughlin, Thulin et al. 2002), suggesting that PhLP may be a regulator of CCT activity or conversely that CCT could control the availability of PhLP during G protein signaling (McLaughlin, Thulin et al. 2002).

To gain further insight into the interaction between CCT and PhLP, we have carried out biochemical analysis of the CCT·PhLP complex. Three-dimensional reconstruction of CCT·PhLP obtained by cryoelectron microscopy together with binding experiments performed with various PhLP mutants has led to the determination of the regions of PhLP and the subunits of CCT involved in the formation of the CCT·PhLP complex, and to an hypothesis of the physiological function of the CCT·PhLP interaction.

EXPERIMENTAL PROCEDURES

Protein preparation – CCT was purified from soluble extracts of bovine testis as described (Martín-Benito, Boskovic et al. 2002). $G\beta_1\gamma_1$ was purified from bovine retina and recombinant rat PhLP, and the PhLP/Pdc chimeric proteins were expressed and purified from *Escherichia coli* as described (Savage, McLaughlin et al. 2000). The CCT·PhLP complexes were formed by incubating CCT and PhLP in a 1:10 molar ratio for 30 min at 25°C. In the case of the CCT·PhLP·antibody immunocomplexes, preformed CCT·PhLP complexes were incubated with anti-CCTδ 8g monoclonal antibody (5:1 antibody:complex molar ratio) for 15 min at 25°C.

Generation of PhLP/Pdc chimeras – The cDNA for wild-type rat PhLP and Pdc with a 3´ c-myc epitope tag were previously constructed in the pET15b vector (McLaughlin, Thulin et al. 2002). The PhLP/Pdc chimeras were made by PCR amplification of two PhLP cDNA fragments from this vector. The fragments were divided at an endonuclease restriction site within the Pdc sequence to be inserted or the PhLP sequence near the replacement point. If the restriction site was within the Pdc insert, fragments were amplified with primers complimentary to the sequence of PhLP at the replacement point with overhangs containing the Pdc sequence including the restriction site. If there was no restriction site within the Pdc insert, then a primer containing complementary nucleotides of PhLP next to the replacement point, the entire Pdc sequence to be inserted, and the additional PhLP sequence up to the restriction site was used. The other primer was complementary to PhLP sequence including the restriction site. Each fragment was then

amplified by pairing these primers with either the T7 forward or reverse primers from pET15b flanking the PhLP cDNA. The fragments were cut at the restriction site, gel purified, and ligated. The full-length chimeras were then PCR-amplified by using the T7 forward and reverse primers and inserted into the pET15b vector by using the *Nco*RI and *Bam*HI restriction sites. For the P193R chimera, the single amino acid substitution was made by using the QuikChange protocol (Stratagene). All constructs were confirmed by DNA sequence analysis.

Binding of PhLP/Pdc chimeras to CCT – Binding of the PhLP/Pdc chimeras to CCT was measured by co-immunoprecipitation and immunoblotting. Purified PhLP/Pdc chimeric proteins (250nM) were added to 10% rabbit reticulocyte lysate in PBS with 0.5mM PMSF and 0.5% Igepal CA-630 detergent (Sigma) in a 100 µl total volume and incubated for 15 min at 4°C. PhLP/Pdc complexes were immunoprecipitated by using an antibody to the C-terminal c-myc tag fused to each chimera and immunoblotted with an antibody to CCTα or Gβγ as described (McLaughlin, Thulin et al. 2002). Intensities of the CCTα bands from the PhLP/Pdc chimera were expressed as a percentage of the CCTα band intensity from the wild-type PhLP immunoprecipitates.

Electron microscopy – All cryoelectron microscopy methods were performed in the laboratory of Dr. Jose M. Valpuesta at the Universidad Autonoma de Madrid, Spain. For cryoelectron microscopy, 5 µl aliquots of a solution containing CCT·PhLP complexes were applied to glow-discharged holey carbon grids for 1 min, blotted for 5 sec, and frozen rapidly in liquid ethane at -180°C. Images were recorded at 20° tilt under

minimum dose conditions in a FEI G^2 FEG electron microscope equipped with a Gatan cold stage operated at 200 kV and recorded on Kodak SO-163 film at X62,000 nominal magnification and between 1.5 and 2.5 μm underfocus. For electron microscopy of negatively stained samples, 5 μl aliquots were applied to glow-discharged carbon grids for 1 min and then stained for 1 min with 2% uranyl acetate. Images were recorded at 0° tilt in a JEOL 1200EX-II electron microscope operated at 100 kV and recorded at X60,000 nominal magnification.

Image processing, two-dimensional averaging and three-dimensional reconstruction– Micrographs were digitized in a Zeiss SCA1 scanner with a sampling window corresponding to 3.5 Å per pixel for vitrified samples. For two-dimensional classification and averaging, top and side views of CCT particles were selected, aligned by using a free-pattern algorithm, and classified by using self-organizing maps as described (Martín-Benito, Boskovic et al. 2002) to separate the PhLP-bound CCT particles from those free of PhLP. The three-dimensional reconstruction of the CCT·PhLP complex was generated from randomly oriented particles whose orientation was determined by using the angular refinement algorithms provided by Spider (Frank 1996). The volumes were generated by using the back-projection method (Guex and Peitsch 1997). No symmetrization was applied to any of the volumes obtained during the iterative procedure. The final resolution was estimated with the 0.5 criterion for the Fourier shell correlation coefficient between two independent reconstructions by using BSOFT (Heymann 2001). Visualization of the volumes was carried out by using AMIRA (http://amira.zib.de).

Modeling of PhLP and docking of the CCT·PhLP complex – The atomic model of PhLP was generated by homology modeling techniques using the sequences and atomic structures of four Pdc proteins (PDB ID codes 2TRC, 1AOR, 1B9Y, and 1B9X) with the DALI comparison algorithm (Holm and Sander 1993) at the SWISS-MODEL server facilities (Guex and Peitsch 1997) (http://swissmodel.expasy.org//SWISS-MODEL.html). The atomic model of PhLP was then fitted manually into the three-dimensional reconstruction of the CCT·PhLP complex by using O (Jones, Zou et al. 1991).

RESULTS AND DISCUSSION

The formation of the CCT·PhLP complex –To confirm the reported interaction of PhLP with CCT and to visualize the CCT·PhLP complexes, purified CCT was incubated in the absence or presence of a 10 molar excess of purified PhLP, and the samples were stained as described in *Experimental Procedures*. Two typical views were observed under the electron microscope: the most common top view revealing the octameric nature of the CCT rings, and the less frequent side view showing the two-ring structure of the chaperonin. The latter view turned out to be the most informative in detecting the absence (Fig. 1*A*) or the presence of PhLP bound to the chaperonin oligomer (Fig. 1*B*), which seems to occur outside the folding cavity. PhLP protrudes from the apical region of the chaperonin in a manner similar to the interaction between CCT and its cochaperonin prefoldin (PFD) (Martin-Benito, Boskovic et al. 2002). However, unlike what happens with PFD, the side views of the CCT·PhLP complex indicate that the interaction between

PhLP and CCT occurs with only one of the chaperonin rings, regardless of the amount of PhLP added to the CCT solution, confirming the predicted 1:1 stoichiometry for the CCT·PhLP complex (McLaughlin, Thulin et al. 2002).

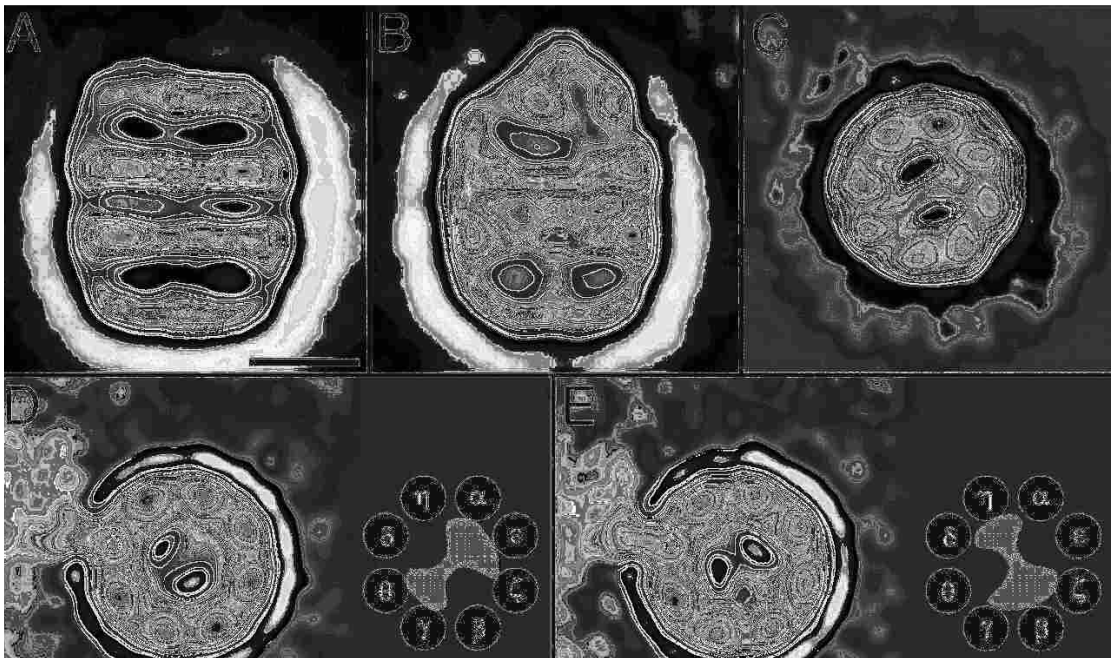

Fig. 2-1. Two dimensional average images of negatively stained CCT·PhLP complex. (*A*) Average image of side views obtained from 243 CCT particles of apo-CCT. (*B*) Average image obtained from 286 side views of CCT·PhLP complexes. (*C*) Average image obtained from 4,225 top views of CCT·PhLP complexes. (*D* and *E*) Average images of the two types of top views of CCT·PhLP·8g (anti-CCTδ) immunocomplexes (average of 324 and 626 particles). The subunit labeled by the antibody is marked with ″δ″ (Scale bar, 100 Å) A schematic model of each mode of PhLP binding, with the topology of the CCT subunits accompanies each average image.

CCT subunits involved in PhLP binding–The side view of the CCT·PhLP complex depicted in Fig. 1*B* also suggests the interaction of PhLP with regions on opposite sides of the CCT cavity. This orientation is confirmed by the average top view image of the same complex (Fig. 1*C*), which shows that an asymmetric mass traverses the chaperonin cavity and interacts with two CCT subunits on one side of the cavity and three CCT subunits on the other side. This interaction is geometry-dependant, similar to what has

already been described for actin (Llorca, McCormack et al. 1999) and tubulin (Llorca, Martín-Benito et al. 2000). To determine whether the interaction is also subunit-specific we made use of a monoclonal antibody reacting against the CCTδ subunit (8g) (Llorca, McCormack et al. 1999). Aliquots of the immunocomplexes were negatively stained (to contrast only one of the CCT rings), and 950 top views were processed. After the classification procedures, two main populations were obtained with PhLP present in the CCT cavity whose average images are represented in Fig. 1*D* and *E*, respectively. Both images reproduce a similar mass crossing the CCT cavity. The specificity of the monoclonal antibody and the known topology of the CCT ring (Liou and Willison 1997) allowed determination of the CCT subunits involved in PhLP binding. The average image shown in Fig. 1*D* represents 65% of the CCT·PhLP complexes and points to an interaction of PhLP with CCTγ/θ on one side of the CCT cavity and CCTα/ε/ζ on the other side. In the average image representing the remaining 35% of the CCT·PhLP complexes (Fig. 1*E*), PhLP seems to interact with CCTδ/η on one side of the cavity and CCTζ/β/γ on the other side. The structural basis for these two different modes of interaction and their physiological relevance remains to be determined. Nevertheless, in either structure PhLP binding occludes the CCT cavity, possibly explaining why PhLP competes with other substrates for their interaction with CCT and therefore regulates the chaperonin folding activity (McLaughlin, Thulin et al. 2002).

Three-dimensional structure of the CCT·PhLP complex–To further characterize the interaction between PhLP and the cytosolic chaperonin, a three-dimensional reconstruction of the CCT·PhLP complex was carried out by cryoelectron microscopy

and image processing. After image classification, a homogenous population of 2,625 particles was obtained and used to generate a three-dimensional reconstruction of the CCT·PhLP complex (Fig. 2*A* and *B*). The reconstruction reveals an asymmetric bullet-shaped structure as was observed in the two-dimensional average image of the side view of the same complex (Fig. 1*B*). Compared with the three-dimensional reconstruction of apo-CCT (Fig. 2*C*), the CCT·PhLP complex shows important differences, especially in the PhLP-bound CCT ring. One difference has to do with the mass clearly attributed to PhLP that sits at the entrance of the cavity and protrudes from it. In contrast to the interaction of CCT with actin (Llorca, McCormack et al. 1999), tubulin (Llorca, Martín-Benito et al. 2000), or its cochaperone, PFD (Martin-Benito, Boskovic et al. 2002), no part of the PhLP mass penetrates into the folding cavity but simply interacts with two opposite sides of the top apical region. The level of resolution of the CCT·PhLP complex (26Å) allows visualization of the PhLP mass as a two-domain structure connected by a small linker. The two domains are clearly asymmetric, the small one interacting with two CCT subunits and the large one with three subunits (Fig. 2*A*). Another difference is a PhLP-induced movement of the apical domains of the CCT subunits, reducing the diameter of the entrance of the folding cavity from ≈80 Å to ≈55 Å and leaving the entrance almost occluded by the presence of PhLP (Fig. 2*A*). This finding confirms the flexibility of the apical domains, which are capable of undergoing large conformational changes within the functional cycle and of accommodating substrates of different sizes (Grantham, Llorca et al. 2000). These large conformational changes of the apical domains induced by PhLP suggest a high-affinity interaction, consistent with the 190 nM K_d reported (McLaughlin, Thulin et al. 2002). The high binding affinity appears to derive

from a concerted action of the two PhLP domains and all eight CCT subunits, probably involving multiple contacts. Finally, the reconstruction also confirms the binding of PhLP to only one of the CCT rings (McLaughlin, Thulin et al. 2002) and strongly suggests that the movement of the apical domains in the PhLP-bound ring transmits an allosteric signal through the equatorial domains so that no PhLP molecule is able to bind to the opposite ring.

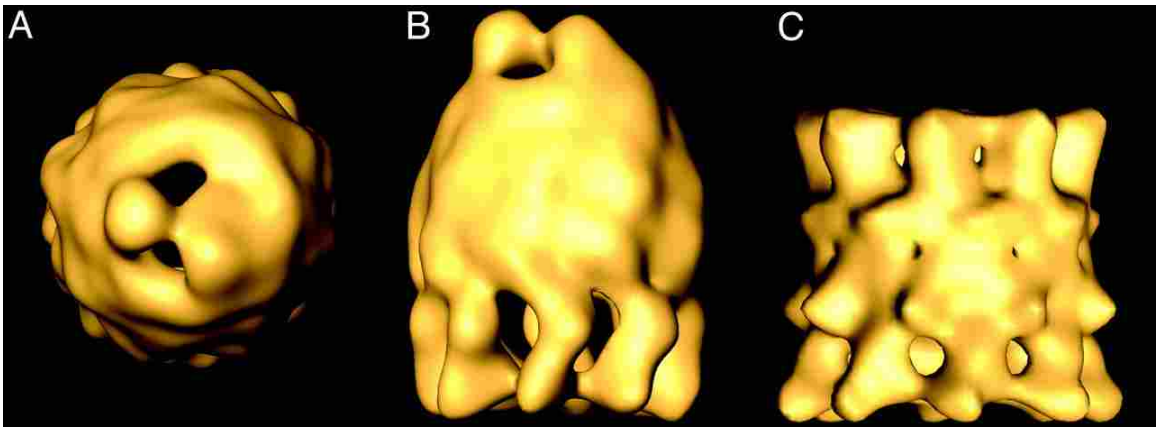

Fig. 2-2. Three-dimensional reconstruction of the CCT·PhLP complex by cryoelectron microscopy. (*A*) Top view of the CCT·PhLP complex. (*B*) Side view of the same volume. (*C*) Side view of the three-dimensional reconstruction of apo-CCT.

Docking analysis of PhLP into the three-dimensional structure of the CCT·PhLP complex–PhLP belongs to a family of widely expressed regulators of G protein signaling (Schroder and Lohse 2000). Although no atomic structure is available for PhLP, there is a high degree of sequence homology between PhLP and Pdc (41% amino acid identity) (Miles, Barhite et al. 1993), another member of the family for which several atomic structures are available (Gaudet, Bohm et al. 1996; Loew, Ho et al. 1998; Gaudet, Savage et al. 1999). This similarity allowed us to generate an atomic model of PhLP by homology modeling techniques (see materials and methods). The atomic model (Fig.3) lacked the first 50 residues of the rat PhLP sequence, which are not present in Pdc, and

the last 24 residues not defined in the atomic structures of Pdc. The model naturally shows very similar structural features to the Pdc atomic structure (Figure 3*B*): an unstructured N-terminal domain built up by three α-helices (H1–H3) and a more compact C-terminal domain showing a typical thioredoxin fold (Martin 1995; Gaudet, Bohm et al. 1996), with a core formed by a five-stranded β-sheet (S1–S5) flanked by four α-helices (H4–H7). The two domains are linked by a flexible loop that connects H3 and S1.

A docking analysis was carried out by fitting the atomic model of PhLP into the mass of the CCT·PhLP complex attributable to PhLP (Fig. 3). The fit is very good only when the C-terminal domain is assigned to the smaller, more compact of the two PhLP masses of the reconstructed volume. The N-terminal domain fits well into the larger mass, and although there is a portion of the mass that is not filled, this could be attributed to the 50 residues of the N-terminal domain not present in the atomic model (red arrow in Fig. 3*B*). An analysis of the docking results suggests the involvement of several regions of PhLP in the binding of CCT (Fig. 3*B* and 3*C*). In the N-terminal domain, a large stretch of amino acids runs parallel to the apical domains of the three CCT subunits that are in close proximity to PhLP (Fig. 3*C*) and suggests a possible binding interface (Fig. 4*A*). This region (K_{109}–E_{135}) encompasses part of the long H1–H2 loop, H2, the H2–H3 loop, and the N-terminal part of H3. In addition, the 50 N-terminal residues not present in the atomic model could potentially be involved in CCT binding through an interaction with the third CCT subunit (red arrow in Fig. 3*B*). In the C-terminal domain, three regions are likely candidates for interaction with the two CCT subunits (Fig. 3*B* and *C*), the loops between S2 and H5 (E_{189}–G_{194}), H6 and S4 (G_{223}–N_{231}), and S5 and H7 (V_{249}–D_{258}). Additionally, part of the last 24 residues of the sequence, not present in the atomic model,

might be placed in the bottom part of the PhLP mass and therefore could also be involved in CCT binding. In all, the electron microscopy shows clearly that both domains of PhLP are involved in CCT binding, and the docking of the atomic model of PhLP into the three-dimensional reconstruction of the CCT·PhLP complex points to several specific regions of both N- and C-terminal domains of PhLP as involved in CCT binding.

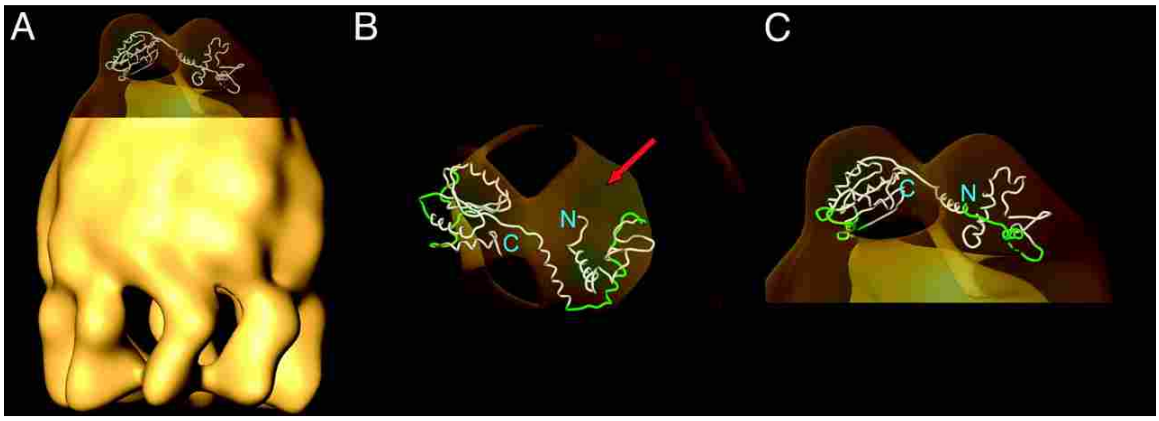

Fig. 2-3. Docking of the atomic model of PhLP into the three-dimensional reconstruction of the CCT·PhLP complex. (*A*) Docking of the atomic model of PhLP into the CCT·PhLP volume. (*B* and *C*) Two enlarged views of the docking of the PhLP atomic model (drawn in tubes) into the CCT·PhLP complex (depicted in transparent fashion). The red arrow in *B* indicates a region of the PhLP mass that could be filled by the 50 residues of the N-terminal sequence of PhLP not present in the PhLP atomic model. The green regions in the atomic model of PhLP are those suggested by the docking analysis to be involved in CCT binding.

Biochemical analysis of the CCT-PhLP interaction–To assess the validity of this structural model of the PhLP-CCT interaction, the binding properties of a set of chimeric proteins were generated in which the PhLP sequences implicated in CCT binding by the cryo-EM studies (Martin-Benito, Bertrand et al. 2004) were replaced with the corresponding Pdc sequence. This mapping strategy takes advantage of the fact that although both proteins are homologous, only PhLP interacts with CCT (McLaughlin, Thulin et al. 2002). A set of two chimeras was generated in which the N-terminal (residues 1–153) and C-terminal (residues 154–301) domains of PhLP were switched

with the corresponding region of Pdc (Fig. 4*A*). The two chimeras were then assayed for CCT and Gβγ binding by co-immunoprecipitation and immunoblotting, the latter serving as a control for the ability of the chimeras to maintain their functional activity and therefore their native conformation. The results in Fig. 4*B* show that neither chimera binds CCT yet both are able to bind Gβγ, indicating that both the N- and the C-terminal domains of PhLP are required for CCT binding. The diminished Gβγ binding of PhLP/Pdc(1–153) is anticipated, given the fact that the N-terminal domain of PhLP contributes more to Gβγ binding than that of Pdc, and that the C-terminal domain of PhLP contributes less than the homologous region of Pdc (Savage, McLaughlin et al. 2000). These results clearly confirm the structural data showing that contacts from both N- and C-terminal domains of PhLP are required for CCT binding.

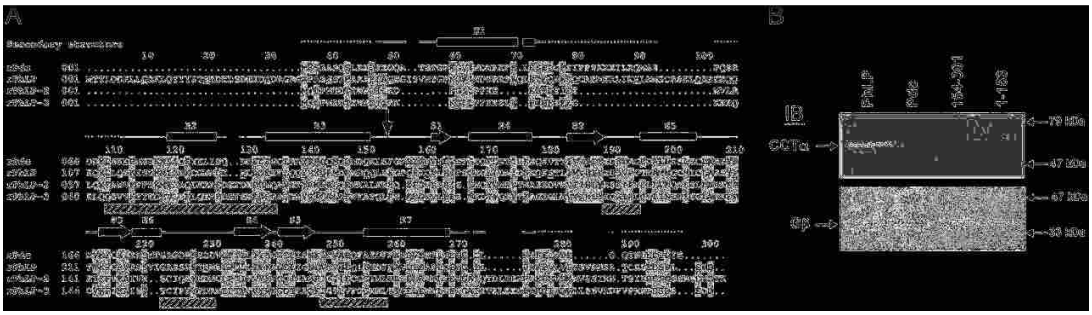

Fig. 2-4. Both domains of PhLP participate in CCT binding. A sequence of alignment of rat Pdc, PhLP1, PhLP2, and PhLP3 is shown in *A*. Conserved residues are indicated with gray boxes, and secondary structural elements for Pdc (Gaudet, Bohm et al. 1996) are indicated above the sequence (H for helix and S for β-strand). Shaded boxes below the structural elements represent regions implicated in CCT binding by the docking analysis. A vertical arrow at residue 154 marks the loop between the N- and C-terminal domains. The PhLP/Pdc(154–301 chimera contains the N-terminal domain of PhLP and the C-terminal domain of Pdc and Vice versa for the PhLP/Pdc(1–153) chimera. In *B*, the binding of these proteins to CCT or Gβ was determined by immunoprecipitation of the PhLP chimeras and immunoblotting for CCTα and Gβ as described in *Materials and Methods.* Immunoblots show representative data from three separate experiments. Positions of molecular weight standards are shown on the right.

The next step was to investigate in detail which specific regions of PhLP are involved in CCT binding, using the information provided by cryo-EM studies (Martin-Benito, Bertrand et al. 2004). Several PhLP/Pdc chimeric proteins were generated in both N- and C-terminal domains of PhLP and were also assayed for CCT and Gβγ binding (Figs. 5 and 6).

In the N-terminal domain, six PhLP/Pdc chimeric proteins were designed to cover most of the secondary structures elements of this domain (Fig. 5*A*): PhLP/Pdc(60–73), in which the putative H1 of PhLP had been switched to the corresponding Pdc sequence; PhLP/Pdc(76–117) and PhLP/Pdc(95–115), covering all or only the C-terminal half of the H1–H2 loop respectively; PhLP/Pdc(116–132), encompassing the last few residues of the H1–H2 loop, H2, and the H2–H3 loop; PhLP/Pdc(130–136), covering the H2–H3 loop and the three N-terminal residues of H3; and finally, PhLP/Pdc(138–154), encompassing H3. The CCT binding assay with the PhLP/Pdc(60–73) chimera showed no decrease with respect to wild-type PhLP (Fig. 5*B*), consistent with cryo-EM studies showing no interaction of H1 with CCT. Binding assays with chimeras PhLP/Pdc(76–117), PhLP/Pdc(95–115), and PhLP/Pdc(116–132) revealed a small decrease in the interaction with the chaperonin (≈20-30%), indicating that the H1–H2 loop, H2, and the N-terminal part of the H2–H3 loop individually make only minor contributions to chaperonin binding. The CCT binding assays with chimeras PhLP/Pdc(130–136) and PhLP/Pdc (138–154) showed a complete suppression of chaperonin binding. The combined information obtained from chimeras PhLP/Pdc(116–132), PhLP/Pdc(130–136), and PhLP/Pdc(138–154) points to H3 and the C-terminal part of the H2–H3 loop as

critical for CCT binding (Fig.5) According to cryo-EM studies, the H2–H3 loop and the N-terminal part of H3 make contact with CCT. In the PhLP/Pdc(130–136) chimera, three nonconservative changes, L131K, E135G, and F136G, abolish CCT binding (Fig. 5), suggesting that the stretch of negative charge D_{132}DEE surrounded by hydrophobic residues is required for CCT binding. Furthermore, in the PhLP/Pdc(138–154) chimera, H3 residues Q_{138}Q that are on the same side of H3 as E_{134}E are replaced with R and K, respectively, increasing the positive charge in this face of H3 (Fig. 5). Interestingly, the negatively charged character of this region is conserved in other PhLP members like PhLP2 and PhLP3 (Fig. 4*A*), which are also believed to interact with CCT (Lacefield and Solomon 2003; Aloy, Böttcher et al. 2004). Indeed, replacement of the D_{132}DEE stretch with alanines in human PhLP abolishes its CCT binding ability (data not shown). Thus, it appears that the negatively charged stretch in the H2–H3 loop and at the N terminus of H3 is critical for CCT binding.

In the C-terminal domain, five chimeras were generated based on the information extracted from the docking analysis (Fig. 6*A*) They were PhLP/Pdc(P193R), in which only a single mutation was necessary to generate the Pdc sequence for the S2–H5 loop; PhLP/Pdc(223–234), encompassing the H6–S4 loop;PhLP/Pdc(249–260), encompassing the S5–H7 loop; and PhLP/Pdc(223–234/249–260), a double-loop chimera switching both of these two later loops. A fifth chimera, PhLP/Pdc(277–301), covered the last 24 residues of the PhLP sequence, a region whose structure was not predicted by the homology modeling experiment but which could be potentially involved in chaperonin binding. The CCT binding assays (Fig. 6*B*) revealed a 60% decrease in chaperonin

binding for PhLP/Pdc(P193R) compared with wild-type PhLP, suggesting that residue P193 is involved in the interaction with CCT, probably through the maintenance of a certain local conformation.

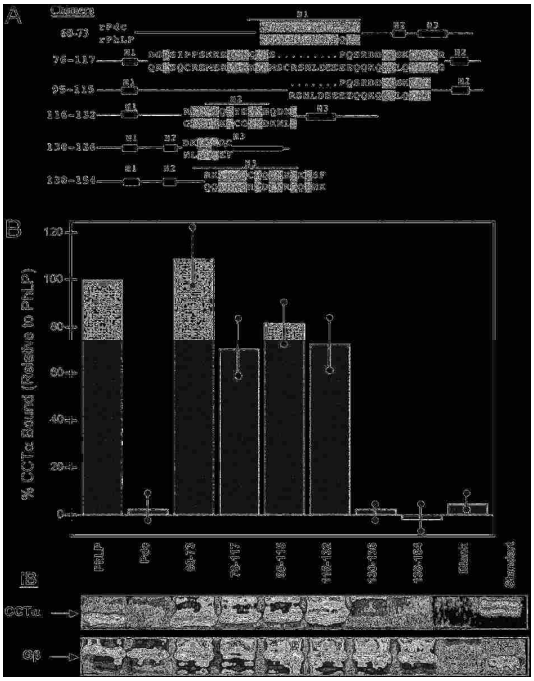

Fig. 2- 5. Binding of PhLP/Pdc chimeras within the N-terminal domain to CCT. Chimeras of PhLP within the N-terminal domain were made by inserting Pdc sequence as shown in *A*. The numbers indicate the residues of PhLP that were replaced with the corresponding Pdc residues and conserved residues within the replacements are located in gray boxes. Binding of these PhLP chimeras to CCT or Gβγ was measured as in Fig. 4. (*B*) Representative immunoblots for CCTα and Gβ, as well as a graphical representation of the CCTα binding data normalized to wild-type PhLP. Bars represent the mean ± standard error from seven separate experiments. No PhLP was added to the blank sample. The standard lanes contain 700 ng of purified CCT (90 ng of CCTα) or 25 ng of Gβγ (21 ng of Gβ).

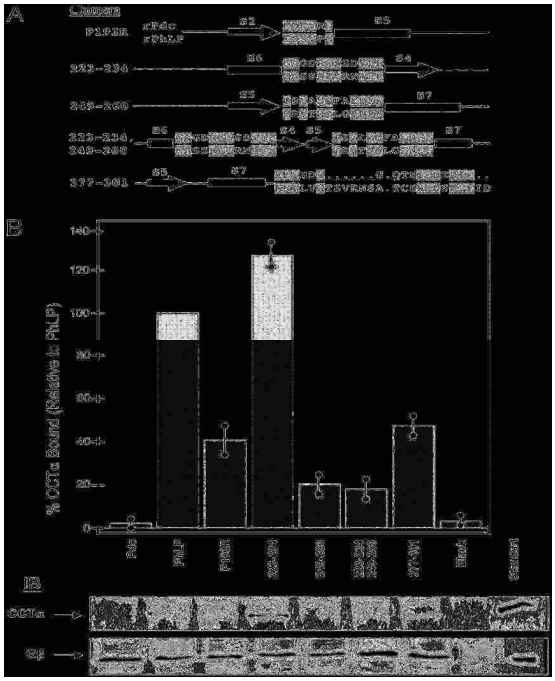

Fig. 2-6. Binding of PhLP/Pdc chimeras within the C-terminal domain to CCT. Chimeras of PhLP within the C-terminal domain were made by inserting Pdc sequence in the loops between the predicted secondary structural elements as shown in *A*. The numbers indicate the residues of PhLP that were replaced with the corresponding Pdc residues and conserved residues within the replacements are located in gray boxes. Binding of these PhLP chimeras to CCT or Gβγ was measured as in Fig. 4. (*B*) Representative immunoblots for CCTα and Gβ, as well as a graphical representation of the CCTα binding data normalized to Wild-type PhLP. Bars represent the mean ± standard error from six separate experiments. The lanes contain the same amounts of protein as in Fig. 5.

Other binding assays showed a small 25% increase in binding with PhLP/Pdc(223–234) and a large 80% decrease in binding with chimera PhLP/Pdc(249–260). A similar 80% decrease was observed for the double-loop chimera PhLP/Pdc(223–234/249–260). These results indicate that the H6–S4 loop is not involved in CCT interaction, whereas the S5–H7 loop has an important role in chaperonin binding. In the PhLP/Pdc (249–260) chimera, there is only one nonconservative substitution (R250S; Fig. 6*A*), suggesting that the positive charge at R250 plays a role in CCT binding. Replacement of the last 24 residues of the C-terminal domain of PhLP with Chimera PhLP/Pdc(277–301) generated a significant 50% decrease in CCT binding, suggesting that this region is also involved in the interaction with the chaperonin.

These biochemical data are generally consistent with the structural model proposed from the docking analysis, confirming most of the suggested contacts and clearly showing that PhLP interacts with CCT through specific regions in both N- and C-terminal domains. In all, the CCT binding experiments shown here suggest that apart from the stringent binding site in the region encompassing part of the H2–H3 loop and H3, PhLP interacts with CCT through the concerted interaction of several regions of both N- and C-terminal domains, similar to what has been described for actin and tubulin (Llorca, McCormack et al. 1999; Llorca, Martín-Benito et al. 2000).

As mentioned earlier, the CCT·PhLP structure displays an interesting similarity to that of the CCT·PFD complex (Martín-Benito, Boskovic et al. 2002) in that PhLP sits above the CCT folding cavity, contacting the apical domains of the CCT subunits and occluding the entrance into the cavity. The function of the co-chaperone PFD is to assist in the folding

of actin and tubulin by binding to their nascent polypeptide chains and delivering them to CCT for folding into their native structures (Martín-Benito, Boskovic et al. 2002). Several lines of evidence suggest a similar role of PhLP with regard to Gβγ folding and/or assembly. First, genetic deletion of PhLP in *Dictyostelium discoideum* blocked G protein signaling and membrane localization of the Gβγ complex (Blaauw, Knol et al. 2003). According to these authors, PhLP could be involved in facilitating the correct folding of Gβ or its assembly into the Gβγ complex. Second, the need of chaperones for the correct folding of WD40 proteins like Gβ has been already demonstrated (Clapham and Neer 1993; García-Higuera, Gaitatzes et al. 1998). Interestingly, the interaction of some of these WD40 proteins with CCT has also been described, and a folding role of CCT has been demonstrated for some of them (Camasses, Bogdanova et al. 2003; Siegers, Bölter et al. 2003). In fact, CCT seems to interact with at least 17% of the yeast WD40 proteins including Ste4, the yeast Gβ subunit (Valpuesta, Martín-Benito et al. 2002). Third, a proteomic analysis of the protein complexes in yeast revealed an interaction between CCT, yeast PhLP2, and VID27, a Gβ protein homologue (Aloy, Böttcher et al. 2004). Fourth, a recent genetic study reveals that the co-chaperoning role of PhLP with respect to CCT could be extended to the folding of β-tubulin (Lacefield and Solomon 2003). In light of these data, it is tempting to suggest that PhLP acts as a co-chaperone in concert with CCT to catalyze the folding of Gβ proteins and/or assembly of the Gβγ complexes.

CHAPTER 3

CK2 MEDIATED ASSEMBLY OF G PROTEIN βγ SUBUNITS BY PHOSDUCIN-LIKE PROTEIN

Introduction–Insight into an alternative function of PhLP has come from the observation that PhLP interacts with the cytosolic chaperonin tailless complex polypeptide 1 (CCT), an essential molecular chaperone that mediates the folding of actin, tubulin, and other proteins into their native structures (McLaughlin, Thulin et al. 2002). PhLP was shown to interact with CCT as a regulator and not as a folding substrate. In addition, the cryoelectron microscopic structure of the PhLP·CCT complex (Martin-Benito, Bertrand et al. 2004) shows that PhLP binds CCT at the top of the CCT apical domains positioned above the folding cavity in a manner analogous to prefoldin, a CCT co-chaperone that binds nascent actin polypeptide chains and delivers them to CCT for folding (Martin-Benito, Boskovic et al. 2002). Coupling these observations with the fact that yeast Gβ (Ho, Gruhler et al. 2002) and other proteins with seven β-propeller structures similar to Gβ (Valpuesta, Martín-Benito et al. 2002; Camasses, Bogdanova et al. 2003; Siegers, Bolter et al. 2003) interact with CCT suggests that PhLP might function as a co-chaperone in the folding of Gβ. Indeed, recent findings show that PhLP does act as an essential chaperone for Gβγ dimer assembly (Lukov, Hu et al. 2005). Specifically, these studies showed that when the expression of PhLP was reduced by 90% in siRNA treated cells, Gβ expression was inhibited by 40% while Gβ mRNA levels remained unaffected. In addition, the siRNA-mediated depletion of PhLP adversely affected G protein signaling, causing a 60% reduction in histamine-induced influx of Ca^{2+} into the cytosol

via a classical Gq-mediated cascade. This reduction in G protein signaling resulted from a decrease in Gβγ assembly in the absence of PhLP. Depletion of PhLP caused a 5-fold decrease in the rate of Gβγ dimer assembly while PhLP over-expression increased Gβγ assembly by 4-fold. Interestingly, over-expression of a truncation of PhLP in which residues 1–75 were deleted (PhLP Δ1–75) revealed that an interaction of PhLP with Gβγ is vital for assembly of the Gβγ dimer. This variant lacks Helix 1, which is known to make a substantial contribution to Gβγ binding (Gaudet, Bohm et al. 1996), yet it retains regions known to interact with CCT (Martin-Benito, Bertrand et al. 2004). This result suggests that a high-affinity binding of PhLP with Gβγ is vital for assembly of the Gβγ dimer but that a high affinity binding of PhLP to CCT may not be necessary when PhLP is overexpressed.

Phosphorylation of PhLP by protein kinase CK2 (CK2) plays an important role in PhLP function. A major site of CK2 phosphorylation occurs within a sequence of three consecutive serines (residues 18–20) near the N-terminus (Humrich, Bermel et al. 2003). Phosphorylation of serines 18–20 was required for PhLP-mediated Gβγ assembly, for when these residues were substituted with alanine, PhLP was unable to catalyze Gβγ dimer formation (Lukov, Hu et al. 2005). The mechanism by which phosphorylation at these sites enhances Gβγ dimer formation is not known; therefore, the effects of CK2 phosphorylation on PhLP function were investigated. The results of these studies provide evidence for a mechanism of PhLP-mediated Gβγ assembly that involves the formation of a ternary complex between PhLP, the nascent Gβ polypeptide, and CCT. PhLP phosphorylation is required for the release of PhLP·Gβ from the CCT complex and the subsequent association of Gγ with Gβ to form the Gβγ dimer. These findings demonstrate

that the physiological function of PhLP is not to down-regulate G protein signaling by sequestering Gβγ but to support G protein signaling by acting as a co-chaperone with CCT in catalyzing Gβγ dimer formation.

EXPERIMENTAL PROCEDURES

Cell Culture – HEK-293 cells and CHO cells were cultured in Dulbecco's modified Eagle's medium/F-12 (50/50 mix) growth media with L-glutamine and 15 mM HEPES, supplemented with 10% fetal bovine serum (HyClone). The cells were subcultured regularly to maintain active growth but were not used beyond 20–25 passages.

Preparation of cDNA constructs – Wild-type human PhLP, PhLP Δ1–75, and Pdc with 3´ c-myc and His_6 tags in the pcDNA3.1/myc-His B vector (Invitrogen) were prepared as described (Lukov, Hu et al. 2005). Serine-to-alanine variants of human PhLP at positions 18, 19, 20, 25, and 296 were constructed in the pcDNA3.1/myc-His B vector by employing a PCR-based strategy and utilizing unique endonuclease restriction sites near the substitution site as described (Lukov, Hu et al. 2005). The constructs were then subcloned into the bacterial expression vector pET15b (Novagen) as described (Carter, Southwick et al. 2004). The integrity of all constructs was confirmed by sequence analysis.

Protein expression and purification – Wild-type and CK2 phosphorylation site variants of human PhLP in the pET15b vector were transformed in *Escherichia coli* DE3 cells and were purified using non-denaturing Ni^{2+} affinity chromatography as described previously (Savage, McLaughlin et al. 2000). The purified proteins were concentrated and

exchanged into 20 mM HEPES, pH 7.2, 150 mM NaCl by ultracentrifugation and were stored in 50% glycerol at –20°C. Protein concentrations were determined using Coomassie Plus protein assay reagent (Pierce), and the purity was determined to be ~95% by SDS-PAGE.

CK2 phosphorylation of PhLP – Purified PhLP (50μM) was phosphorylated by CK2 (10 units/μl, Calbiochem) in 20 mM HEPES, pH 7.5, 100 mM KCl, 20 mM NaCl, 5 mM dithiothreitol, and 1 mM ATP for 1 hr at 37°C. The phosphorylation was confirmed by SDS-PAGE using 10% gels.

Assay of PhLP binding to CCT – The binding of CK2 phosphorylated PhLP and its CK2 phosphorylation site variants to CCT was measured by adding 5 nM purified PhLP to 5% rabbit reticulocyte lysate in phosphate-buffered saline containing 1.2% IGEPAL CA-630 (Sigma) and 0.6 mM phenylmethylsulfonyl fluoride in a total volume of 300 μl. Binding was allowed to proceed for 30 min at 23°C after which the PhLP was immunoprecipitated by incubating for 30 min at 4°C with 2.1 μg of anti-c myc antibody (clone 9E10, Biomol) followed by the addition of 30 μl of a 50% slurry of Protein A/G Plus-agarose beads (Santa Cruz Biotechnology) and another 30-min incubation at 4°C with constant mixing. The beads were washed with the phosphate-buffered saline/IGEPAL buffer, and proteins were solubilized with 20 μl of 2X SDS-PAGE sample buffer. 15 μl of each sample was resolved on a 10% SDS-PAGE gel and was immunoblotted with a 1:1000 dilution of rabbit polyclonal anti-CCTε antiserum (Martin-Benito, Bertrand et al. 2004) followed by a 1:2000 dilution of goat anti-rabbit horseradish peroxidase-conjugated secondary antibody (Calbiochem). Immunoblots were developed with the ECL Plus chemiluminescence reagent (GE Healthcare) and visualized with a

storm 860 PhosphorImager (Amersham Biosciences). The band intensities were quantified using Image-QuaNT software (Amersham Biosciences).

Assay of PhLP inhibition of G_t binding to rhodopsin – Light-induced binding of 0.2 μM ^{125}I-labeled $G_t\alpha$ and 0.2 μM $G_t\beta\gamma$ to membranes containing 1 μM rhodopsin ± 2 μM CK2 phosphorylated or unphosphorylated PhLP was measured as described previously (Savage, McLaughlin et al. 2000).

Mass spectrometric analyses – Tryptic peptides of CK2-phosphorylated PhLP were generated and analyzed as described previously (Carter, Southwick et al. 2004). Briefly, molecular ions in the effluent from a C18 capillary chromatography that correspond to the predicted masses of phosphopeptides from PhLP were fragmented by collision-induced dissociation in a Q-ToF mass spectrometer (LC/MS/MS). Fragmentation spectra were obtained using either automated or manual parent ion selection. Data were analyzed using BioAnalyst software (Applied Biosystems, Farmingham, MA).

Electrophoretic mobility determinations – CHO cells were plated in 6-well plates so that they were 70–80% confluent the next day. The cells were then transfected with 1 μg of either wild-type PhLP-myc or one of the CK2 phosphorylation site variants using Lipofectamine Plus reagent (Invitrogen) according to the manufacturer's protocol. The cells were harvested 48 hr later in 200 μl of immunoprecipitation buffer (Lukov, Hu et al. 2005), and the PhLP-myc was immunoprecipitated from the lysate with 3 μg of anti-c-myc antibody and 30 μl of protein A/G beads as described previously (McLaughlin, Thulin et al. 2002; Lukov, Hu et al. 2005). The final precipitate was solubilized in 40 μl of 2X SDS-PAGE sample buffer, and 10 μl of each sample was resolved on 10% SDS-

PAGE gels. The gels were immunoblotted with a 1:1000 dilution of the anti-c-myc antibody and developed as described above.

Gβγ expression measurements – HEK-293 cells were plated in 6-well plates so that they would be 70-80% confluent the following day. They were then co-transfected with 1 μg of each of the PhLP-myc, HA-$G\gamma_2$, and $G\beta_1$ cDNAs using Lipofectamine Plus reagent. In all experiments involving multiple transfections, the total amount of cDNA was held constant by adding empty vector. After 48 h, the cells were washed and solubilized in 200 μl of immunoprecipitation buffer. The $G\beta_1\gamma_2$ complexes were immunoprecipitated from 100 μl of the lysate with 1.5 μg of anti-HA (clone 3F10, Roche Applied Science) antibody as described previously (McLaughlin, Thulin et al. 2002; Lukov, Hu et al. 2005). The complexes were solubilized in 40 μl of 2X SDS sample buffer, and 10 μl was resolved on 10% Tris-Tricine SDS-PAGE gels for $G\beta_1$, or 20 μl was resolved on 16.5% Tris-Tricine SDS-PAGE gels for $G\gamma_2$. For Gβ detection, the gels were immunoblotted with a 1:2000 dilution of a $G\beta_1$ antibody in the blocking buffer and then 1 h in a 1:2000 dilution of goat anti-rat horseradish peroxidase-conjugated secondary antibody (Calbiochem). The immunoblots were developed as described above.

Radiolabel pulse-chase assay – The pulse-chase assay was performed and quantified as described previously (Lukov, Hu et al. 2005). A similar protocol was used to measure the rate of release of nascent Gβ from CCT. Six-well plates of HEK-293 cells were cotransfected with 1 μg of FLAG $G\beta_1$, HA-$G\gamma_2$ or PhLP-myc variants as indicated. After a 10-min pulse, the radiolabel was chased for the times indicated and the cells were harvested in 220 μl of immunoprecipitation buffer. The extract was divided into two 95

µl samples, and 2.5 µl of 1 µg/µl anti-CCTε antibody (Serotec) was added to one sample and 3.0 µl of 1 µg/µl anti-FLAG antibody was added to the other sample. The immunoprecipitation and analysis of the radiolabeled proteins co-immunoprecipitating with CCT were carried out as described (Lukov, Hu et al. 2005). The $G\beta_1$ band was clearly separated from the other radiolabeled bands, facilitating its quantification. The amount of $G\beta_1$ in the CCT immunoprecipitate was divided by that in the FLAG-$G\beta_1$ immunoprecipitate to determine the fraction of the total $G\beta_1$ bound to CCT. These values were expressed as a percentage of the 30-min time point to readily compare the rates of Gβ dissociation from CCT. The data were fit to a first order dissociation rate equation using the KaleidaGraph graphics software to determine the dissociation rate constant *k*. From the *k* values, the half-life was calculated by the equation, $t_{1/2} = \ln 2/k$.

Assay of Gβ binding to CCT – For CCT binding experiments involving $G\beta_1$ overexpression, HEK-293 cells were plated in 6-well plates and transfected with 1.0 µg of PhLP variants, and 1.5 µg of HA-Gγ as indicated in Fig. 5 (*A* and *C*). Alternatively, the transfections were performed with 0.5 µg of FLAG-$G\beta_1$, 1.0 µg PhLP variants, and 1.5 µg of HA-Gγ as indicated in Fig 6*A*. After 48 h, cells were lysed and extracts were immunoprecipitated with 2.5 µg of anti-CCTε antibody (Serotec), the immunoprecipitates were resolved on SDS-PAGE gels and immunoblotted for FLAG-$G\beta_1$, PhLP-myc, Pdc-myc, or HA-$G\gamma_2$ using the indicated antibodies as described above, the intensities were calculated as a percentage of the control as indicated.

For binding experiments involving endogenous Gβ, HEK-293 cells were grown in 100-mm dishes and transfected with 6.0 µg of PhLP variant cDNAs as indicated in Fig. 5*B*.

Cells were lysed in 1.2 ml of buffer, and 1 ml was immunoprecipitated with 10 μg of anti-CCTε antibody and 60 μl of protein A/G beads. Endogenous $G\beta_1$ was detected with the anti-$G\beta_1$ antibody. For binding experiments involving endogenous PhLP, HEK-293 cells were grown in 6-well plates and transfected with 1.0 μg of FLAG-$G\beta_1$ cDNA as indicated in Fig. 5*C*. Extracts from two wells were pooled, and 200 μl was immunoprecipitated with 3 μg of anti-CCTε antibody. Other immunoprecipitation and immunoblotting procedures were as described above.

RESULTS

Effects of CK2 phosphorylation of PhLP on CCT and Gβγ binding–To begin to assess the impact of CK2 phosphorylation on PhLP function, the effects of phosphorylation on the binding of PhLP to its two known binding partners, Gβγ and CCT, were determined *in vitro*. Purified recombinant human PhLP was readily phosphorylated by CK2, resulting in a marked reduction of the mobility of the PhLP protein band in SDS-PAGE gels (Fig. 1*A*). The entire PhLP band was shifted, indicating that phosphorylation was 100% complete under the conditions used. The effects of CK2 phosphorylation on CCT binding was assessed by measuring the ability of PhLP to co-immuno-precipitate CCT from rabbit reticulocyte lysate (Martin-Benito, Bertrand et al. 2004). Human PhLP bound CCT with a high affinity, as evidenced by the fact that addition of 5 nM PhLP was sufficient to co-immuno-precipitate readily detectable amounts of CCT from rabbit reticulocyte lysate. Under these conditions, CK2 phosphorylation increased the co-immunoprecipitation of CCT by 7-fold (Fig. 1*B*). In contrast, CK2 phosphorylation had no effect on the ability of

PhLP to co-immunoprecipitate purified Gβγ (Fig. 1*B*) or to inhibit association of $G\beta_1\gamma_1$ with $G_t\alpha$ and light-activated rhodopsin (Fig. 1*C*), indicating that phosphorylation did not change the binding of PhLP to $G\beta_1\gamma_1$.

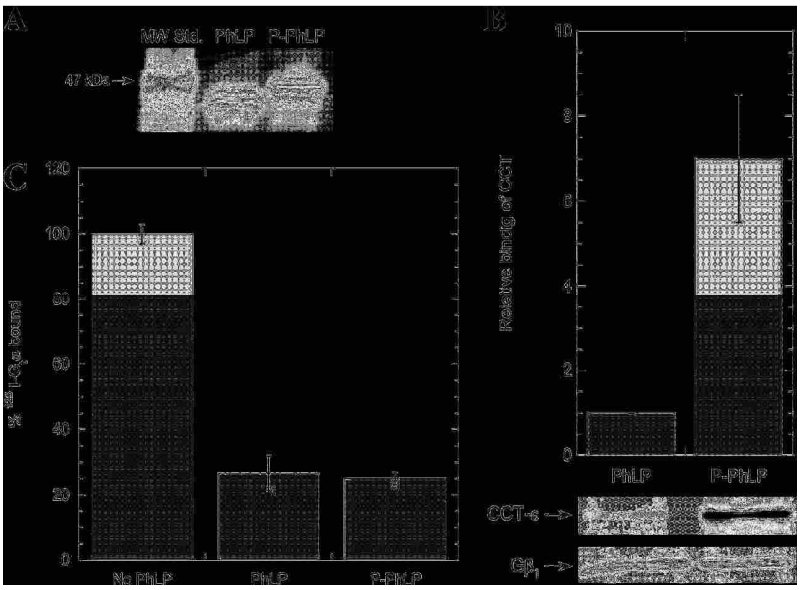

Fig. 3-1. **Effects of CK2 phosphorylation on PhLP binding to CCT and Gβγ**. (*A*) The decrease in mobility of PhLP in SDS-PAGE upon CK2 phosphorylation is shown. PhLP was phosphorylated by CK2 *in vitro* (*P-PhLP*) and was analyzed on a 10% gel along with unphosphorylated PhLP. (*B*) The effects of CK2 phosphorylation on the binding of PhLP to CCT and Gβγ are shown. Binding was measured by immunoprecipitation of PhLP coupled with detection of the co-immunoprecipitating CCTε or Gβ by immunoblotting. A representative immunoblot is shown. The graph gives the average intensity ± standard error of the CCT bands relative to the unphosphorylated sample from eight separate experiments. (*C*) The effects of CK2 phosphorylation on the ability of PhLP to inhibit $G\beta_1\gamma_1$-assisted binding of ^{125}I-labeled $G_t\alpha$ to membranes containing light-activated rhodopsin were determined. The graph gives the average ± standard error from three separate experiments.

Mass spectrometric analysis of the CK2 phosphorylation sites of PhLP – The phosphorylation sites that could potentially be responsible for the increase in PhLP binding to CCT upon CK2 phosphorylation were identified by mass spectrometry. PhLP was phosphorylated by CK2 *in vitro* and digested with trypsin, and the resulting peptide fragments were analyzed by electrospray tandem mass spectrometry. All mass spec

experiments were performed by Michael Carter and Craig Thulin, and included for completeness. Fig 2 shows the collision induced dissociation (CID) spectrum of a doubly charged parent ion with an *m/z* ratio of 1198.5, corresponding to the mass of a tryptic peptide containing the C-terminal residues 287–301 of PhLP plus one phosphate. This CID spectrum showed robust peaks for both the b and y ions corresponding to the sequence of the 287–301 peptide. Of these, the y16 ion had an *m/z* equal to the loss of a phosphate, and the formation of a dehydroalanine at one of the two serines in this fragment, indicating that either Ser-293 or Ser-296 was phosphorylated in the parent ion. The b2, b4, b6, and b9 ions all had *m/z* ratios corresponding to the mass of their unphosphorylated fragments, suggesting that Ser-288 and Ser-293 were not phosphorylated. Therefore, the phosphate most likely resided on Ser-296. Accordingly, Ser-296 is within a strong consensus site for CK2 phosphorylation with negatively charged residues at the +1 and +3 positions (Meggio and Pinna 2003).

One other tryptic fragment with *m/z* values corresponding to a phosphorylated species was detected and analyzed by CID. This peptide consisted of PhLP residues 13–32 plus one and two phosphates. The spectrum for the singly phosphorylated species yielded few b and y ions, none of which were phosphorylated. However, there were sufficient fragments to confirm the identity of the peptide (Fig. 2*B*). The same result was obtained with the doubly phosphorylated species. The CID spectrum confirmed the identity of the peptide but did not show any phosphorylated fragments (Fig. 2*C*). Hence, the four serines of this peptide, serines 18–20 and 25, could all be considered as potential CK2 phosphorylation sites.

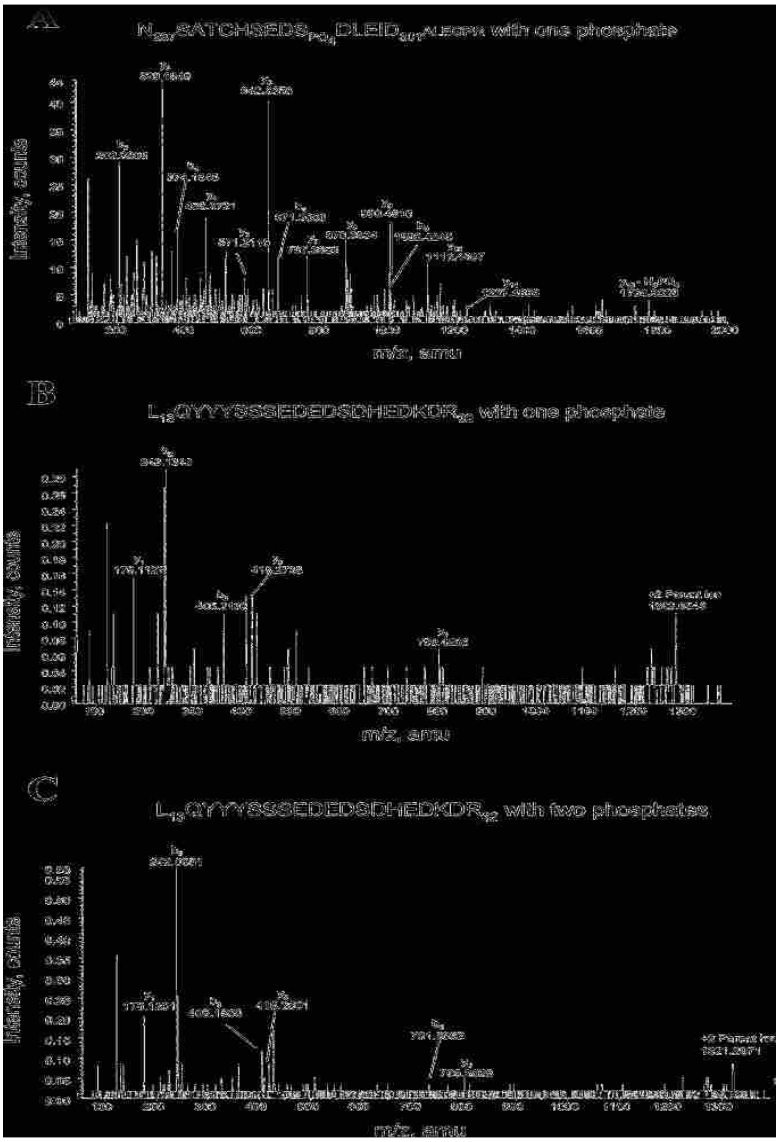

FIG. 3-2.Mass spectrometric analysis of the CK2 phosphorylation sites of PhLP. (*A*) PhLP was phosphorylated by CK2 *in vitro* and digested with trypsin, and the resulting peptide fragments were analyzed by LC/MS/MS. CID spectrum of the +2 parent ion corresponding to the *m*/*z* of the C-terminal sequence of PhLP plus one phosphate are indicated above the spectrum. The PhLP sequence ends at Asp-301, and the additional residues (*smaller font*) are part of the linker for the C-terminal *myc* tag of the recombinant human PhLP. The *m*/*z* values corresponding to the b and y ions resulting from fragmentation of this peptide are indicated. The 1764 *m*/*z* peak corresponds to the y16 ion with one dehydroalanine generated from the loss of H_3PO_4 from a phosphoserine during fragmentation. (*B*) CID spectrum of the +2 parent ion corresponding to the *m*/*z* of residues 13-32 of PhLP plus one phosphate. The *m*/*z* values corresponding to the b and y ions resulting from fragmentation of this peptide are indicated. (*C*) CID spectrum of the +2 parent ion corresponding to the *m*/*z* of residues 13-32 of PhLP plus two phosphates. The *m*/*z* values corresponding to the b and y ions resulting from fragmentation of this peptide are indicated.

Of the four, Ser-20 and Ser-25 are within CK2 consensus sites, and phosphorylation of Ser-20 would create a strong consensus site for CK2 phosphorylation of Ser-19 in a doubly phosphorylated species. Similarly, phosphorylation of Ser-19 would make Ser-18 a good CK2 site, although no triply phosphorylated species of the 18–32 peptide were detected. Together, the mass spectrometric data suggest five potential CK2 phosphorylation sites on PhLP: Ser-18, Ser-19, Ser-20, Ser-25, and Ser-296.

Contribution of specific CK2 phosphorylation sites to the PhLP-CCT interaction – To identify which of these sites is responsible for the phosphorylation-dependant increase in PhLP binding to CCT, each of the five serines identified above was substituted with alanine in various combinations. The resulting PhLP variants were CK2-phosphorylated, and their binding to CCT was determined as described in Fig. 1. Substitution of one residue within the serine 18–20 sequence caused only minor reductions in the phosphorylation-induced increase in binding, whereas substitution of two residues within this sequence resulted in reductions in the phosphorylation-induced binding from 7-fold to ~4 fold (Fig. 3). Replacement of all three serines within this phosphorylation site caused a further reduction in the phosphorylation-induced increase to 3-fold, indicating that multiple phosphorylation events within the serine 18–20 sites were responsible for much of the observed increase in PhLP binding to CCT upon CK2 phosphorylation. With regard to the Ser-25 and Ser-296 sites, replacement of both residues caused a similar modest decrease in binding as was seen with dual substitution within the serine 18–20 site, while replacement of either Ser-25 or Ser-296 along with all three of the Ser-18, Ser-19, and Ser-20 residues was required to completely block the phosphorylation-induced increase in binding.

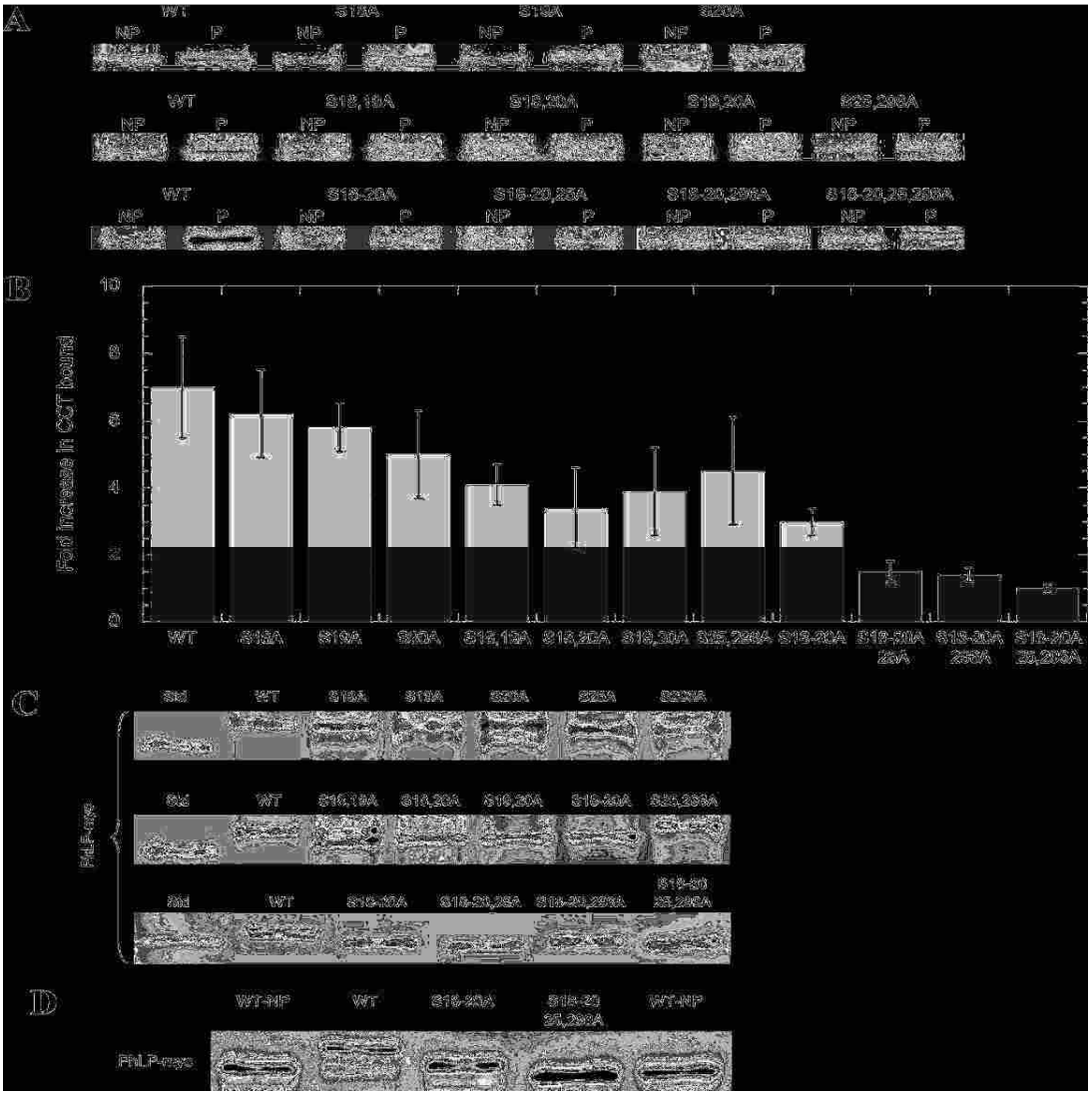

FIG. 3-3.Contribution of specific CK2 phosphorylation sites to the PhLP·CCT interaction. (*A*) phosphorylation-induced increase in PhLP binding to CCT is shown for several PhLP variants with the serine-to-alanine substitutions indicated. Binding of CCT to PhLP was determined for each variant as in Fig. 1. Representative immunoblots for the phosphorylated (*P*) and unphosphorylated (*NP*) variants are shown. (*B*) The -fold increase in CCT bound upon CK2 phosphorylation of PhLP was calculated by dividing the CCTε band intensity of the phosphorylated sample by that of the unphosphorylated sample. The graph gives the average increase ± standard error from three to five separate experiments. (*C*) The shift in electrophoretic mobility of PhLP upon CK2 phosphorylation was used to determine which of the putative CK2 sites were phosphorylated in cells. CHO cells were transfected with the indicated PhLP variants with C-terminal myc epitope tags. After 48 h, the cells were harvested and extracts were immunoprecipitated and immunoblotted with an antibody to the myc tag. Phosphorylation of the variants was determined by the shift in mobility of the PhLP band compared with wild-type PhLP-myc or purified, unphosphorylated PhLP-myc. *(D*) The electrophoretic mobility of wild-type PhLP and the indicated PhLP variants after CK2 phosphorylation *in vitro* was also determined to compare the mobility shifts *in vitro* with those observed in cells. PhLP variants were analyzed by SDS-PAGE gels as in Fig. 1.

These results show that each of the five serines identified by mass spectrometry can contribute to the phosphorylation-induced increase in PhLP binding to CCT and that no other CK2 phosphorylation sites are involved in this process, suggesting that all the major CK2 phosphorylation sites were identified in the mass spectrometric analysis.

It is important to note that the serine to alanine replacements did not change the binding of unphosphorylated PhLP to CCT significantly (Fig. 3*A*), indicating that the alanine substitutions did not affect the folding of the PhLP variants nor did they modify the PhLP-CCT interaction significantly. Thus, the loss of the phosphorylation-induced increase in binding with the multiple alanine substitutions could be attributed to an inability of the variants to be phosphorylated by CK2.

Identification of specific CK2 phosphorylation sites in cells–To assess whether the CK2 phosphorylation sites of PhLP identified *in vitro* were also phosphorylated *in vivo*, the decrease in electrophoretic mobility upon CK2 phosphorylation was exploited to detect PhLP phosphorylation events in living cells. This work was completed by Georgi Lukov and is included for completeness. In this experiment, PhLP serine to alanine substitution variants with a C-terminal myc tag were transfected into CHO cells. Cells were extracted, and the PhLP was immunoprecipitated and immunoblotted with an antibody to the tag to distinguish the variants from the endogenous PhLP. Substitution of a serine that normally would be phosphorylated by CK2 in wild-type PhLP would be expected to result in an increase in mobility of that PhLP variant. Wild-type PhLP showed decreased mobility of the entire band when compared with an unphosphorylated PhLP standard, indicating that all of the transfected PhLP was phosphorylated in the CHO cells (Fig. 3*C*, *upper panel*). The PhLP S20A variant showed two bands, a higher band with the same mobility as

wild-type PhLP and a lower band with increased mobility. The ratio of the intensities of the two bands was ~2 to 1, with the higher band having the greater intensity. The PhLP S18A and S19A showed a very small amount of the lower band, whereas S25A and S296A showed no lower bands. The presence of both bands in the S20A variant suggests that phosphorylation of Ser-18 or Ser-19 may be partially impaired when position 20 cannot be phosphorylated. These results indicate that Ser-20 is phosphorylated in cells and that other phosphorylation events might also occur within the serine 18–20 sequence.

A similar analysis was done with double and triple serine to alanine substitutions (Fig. 3*C*, *middle panel*). The S18A/S19A/S20A variant showed a single lower band compared with wild-type PhLP but that was still higher than the unphosphorylated control. The S18A/S20A and S19A/S20A variants also showed a major lower band, with almost no higher band corresponding to wild-type PhLP. The S18A/S19A variant showed both the higher and lower bands, confirming phosphorylation at Ser-20 and indicating that it is sufficient for the mobility shift. The two bands also suggest that Ser-20 phosphorylation may be impaired in the absence of serine or phosphoserine at position 18 or 19. In the case of the S25A/S296A variant, there was a single higher band with the same mobility as wild-type PhLP, demonstrating that the large decrease in mobility is not a result of Ser-25 or Ser-296 phosphorylation, but rather it stems from at least one phosphorylation event in the Ser-18, Ser-19, and Ser-20 sequence.

The mobility of PhLP variants substituted at four and all five sites was also determined. The S18A/S19A/S20A/S25A variant causes an additional increase in the mobility of the PhLP band to the same mobility as unphosphorylated PhLP, whereas the S18A/S19A/S20A/S296A variant did not increase the mobility beyond that of serines 18–

20. The variant in which all five sites were substituted has the same mobility as the S18A/S19A/S20A/S25A variant and unphosphorylated PhLP. These data show that Ser-25 is also phosphorylated in cells, at least in the absence of phosphorylation at serines 18–20, and that Ser-25 phosphorylation causes a small decrease in PhLP mobility. The lack of change in mobility with substitution of Ser-296 did not permit a conclusion to be made about the phosphorylation of this site in cells. Either phosphorylation at Ser-296 did not occur or it did not change the mobility of PhLP in SDS gels.

A very similar pattern of electrophoretic mobility shifts was observed with *in vitro* CK2 phosphorylation of the PhLP S/A variants (Fig. 3*D*). S18A/S19A/S20A showed increased mobility compared with wild-type PhLP, and the S18A/S19A/S20A/S25A/S296A variant had the same mobility as unphosphorylated PhLP. The similarities in mobility of the PhLP variants between the *in vitro* phosphorylation and that found in cells argue that CK2 is responsible for PhLP phosphorylation *in vivo*, in agreement with previous data indicating that CK2 was the physiologically relevant kinase (Humrich, Bermel et al. 2003). Importantly, in the absence of CK2 phosphorylation, the S/A variants all had the same mobility as unphosphorylated wild-type PhLP (data not shown), indicating that the differences in mobility were not caused by the alanine substitutions. Together, these data make a strong case for CK2 phosphorylation events within the serines 18–20 and 25 sites *in vivo*.

Effects of specific CK2 phosphorylation sites on Gβγ expression and dimer assembly–It has recently been reported that substitution of all three serine residues in the serine 18–20 sequence blocked the ability of PhLP to enhance the cellular expression of Gβγ

(Humrich, Bermel et al. 2005; Lukov, Hu et al. 2005). To further investigate this phenomenon, the CK2 phosphorylation site variants of PhLP were coexpressed with $G\beta_1$ and $G\gamma_2$ in HEK-293 cells, and the effects on Gβγ expression were measured by immunoprecipitating the $G\gamma_2$ from cell extracts and immunoblotting for both $G\beta_1$ and $G\gamma_2$. This work was performed by Georgi Lukov, and is included for the purpose of completeness. Co-expression of the single phosphorylation site variants did not change Gβγ expression significantly compared with wild type, nor did co-expression of the S18A/S19A or the S25A/S296A double variants (Fig. 4, *A* and *B*). However, co-expression of the S18A/S20A or the S19A/S20A double variants inhibited Gβ expression by 60-70% and Gγ expression by ~50% compared with wild type (Fig. 4*A*). Likewise, the S18A/S19A/S20A triple variant inhibited Gβ and Gγ expression by 70-80% and 60-70%, respectively (Fig. 4, *A* and *B*). Further substitution of Ser-25 and Ser-296 caused no further decreases in Gβγ expression (Fig. 4*B*). These data clearly show that phosphorylation of at least one serine within the serine 18–20 sequence is important for PhLP to assist in the expression of Gβγ, with Ser-20 phosphorylation contributing the most to this process. They also show that phosphorylation of Ser-25 and Ser-296 plays no additional role in Gβγ expression. Moreover, the significant reduction in Gβγ expression by several of the PhLP serine 18–20 variants to levels below those observed with the empty vector indicate that these variants block the ability of endogenous PhLP to support Gβγ expression and are thus acting as dominant negative inhibitors of Gβγ.

The reason for enhanced Gβγ expression in the presence of CK2-phosphorylated PhLP is that phosphorylated PhLP increases the rate of Gβγ dimer assembly (Humrich, Bermel et

al. 2005; Lukov, Hu et al. 2005). To determine which phosphorylation sites are critical for PhLP-mediated Gβγ assembly, the ability of the PhLP CK2 phosphorylation site variants to catalyze Gβγ dimer assembly was determined. All of the double and triple variants of the serine 18–20 sequence were compromised in their ability to assist in Gβγ dimer formation compared with wild-type PhLP (Fig. 4*C*). The S18A/S19A variant was the least compromised, as reflected by an assembly half-life of 99 min compared with 42 min for wild-type PhLP, whereas the S18A/S19A/S20A variant was the most compromised, with a half-life of 284 min (Fig. 4*C*). The S19A/S20A and S18A/S20A variants showed intermediate half-lives of 153 and 128 min, respectively. In contrast, the S25A/S296A variant was as effective as wild-type PhLP in promoting Gβγ assembly with a half-life of 46 min. These Gβγ assembly results are qualitatively similar to the Gβγ expression data. However, there is one significant quantitative difference in the S18A/S19A variant between the Gβγ expression and the Gβγ assembly data. Gβγ expression was only slightly reduced by the S18A/S19A variant, whereas the rate of Gβγ assembly was reduced by >2-fold. This difference can be explained by the 48 hr time period over which Gβγ expression was measured. It appears that the 2-fold reduction in the rate of Gβγ assembly is sufficient to maintain the steady-state Gβγ levels achieved in the 48 hr expression period to near those found in the presence of wild-type PhLP, whereas the larger reduction in assembly observed with the other Ser-18, Ser-19, and Ser-20 variants is not. Together, the Gβγ assembly and expression data indicate that two phosphorylation events in the serine 18–20 sequence are required for PhLP to be fully active in catalyzing Gβγ assembly. Phosphorylation at one of the three sites results in

partial activity, with Ser-20 phosphorylation conferring the most activity. The results also show that phosphorylation of Ser-25 or Ser-296 has no bearing on Gβγ assembly.

Gβ Binds CCT in a Ternary Complex with PhLP–The correlation between the increase in binding of PhLP to CCT upon phosphorylation of serines 18–20 (Fig. 3*B*) and the necessity of phosphorylation of serines 18–20 for full activity in Gβγ assembly (Fig. 4*C*) suggests that the effects of PhLP phosphorylation on assembly may occur through CCT. However, a role for CCT in Gβγ assembly has not been established (Humrich, Bermel et al. 2005; Lukov, Hu et al. 2005). If CCT does participate in the assembly process, then it must interact with Gβ, Gγ, or both. An interaction between Gβ and CCT has been observed in yeast protein interaction screens, but no such interaction has been reported in mammalian cells. Therefore, the binding of Gβ and Gγ to CCT was assessed by co-immunoprecipitation of overexpressed Gβ or Gγ in HEK-293 cells. This work was performed by Christine Baker, and is included for the purpose of completeness. Gβ co-immunoprecipitated with CCT robustly, to a similar extent as overexpressed PhLP, whereas overexpressed Pdc, which does not bind CCT, was not found in the CCT immunoprecipitate (Fig. 5*A*). Thus, Gβ appears to be specifically interacting with CCT under overexpression conditions. In contrast, over-expressed Gγ did not co-immunoprecipitate with CCT (Fig. 5*A*). To determine whether the interaction also occurred with endogenous amounts of Gβ, the experiment was also done without overexpressing Gβ. Co-immunoprecipitation of Gβ with CCT was also observed with endogenous Gβ, confirming the results of the overexpression experiments (Fig. 5*B*).

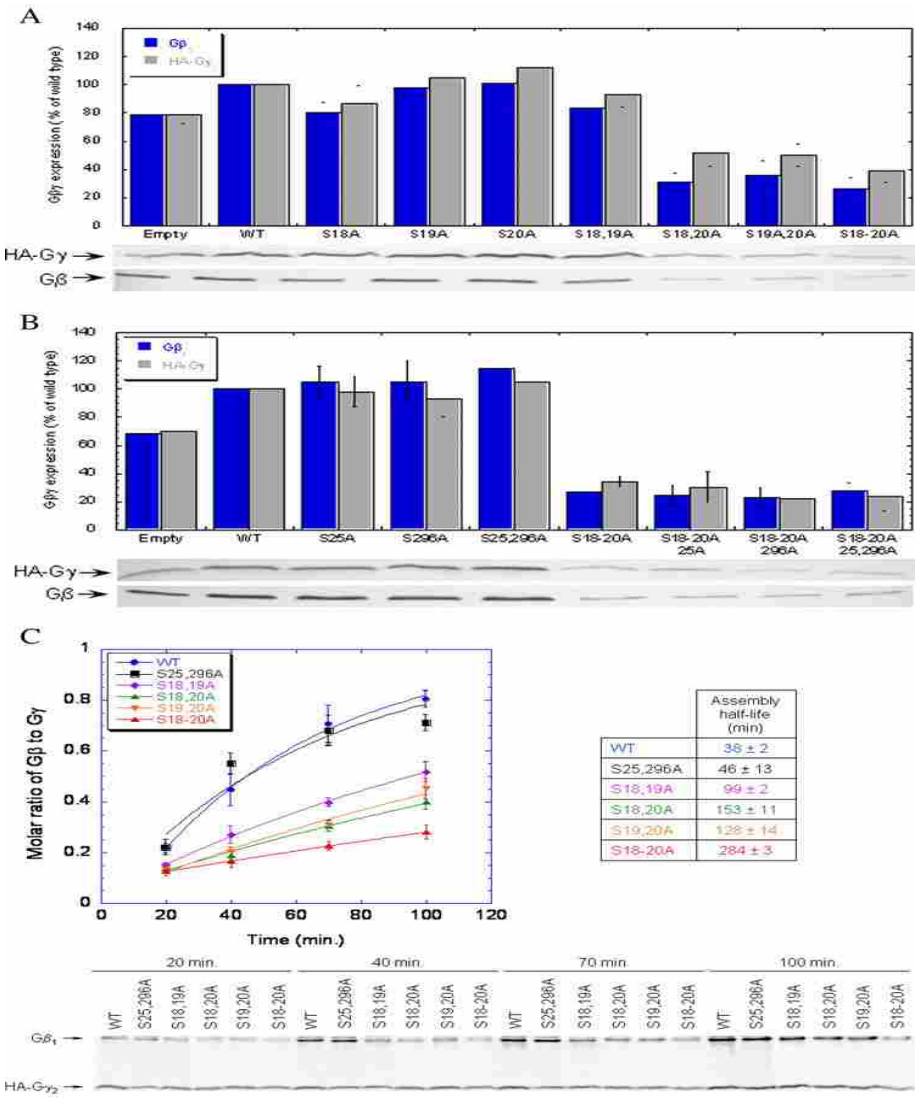

FIG. 3-4. **Effects of PhLP phosphorylation on Gβγ expression and assembly.** (*A*) Cellular expression of Gβγ dimers was determined in the presence of PhLP S18A/S19A/S20A variants. HEK-293 cells were transfected with $G\beta_1$, HA-tagged $G\gamma_2$, and the indicated variants. The cells were harvested, and extracts were immunoprecipitated with an antibody to the HA tag. The amount of HA-$G\gamma_2$ and co-immunoprecipitated $G\beta_1$ was determined by immunoblotting with anti-HA and anti-$G\beta_1$ antibodies. A representative blot is shown. The *graph* gives the average $G\beta_1$ and HA-$G\gamma_2$ amounts ± S.E. relative to wild-type PhLP from three separate experiments. Cells in the empty sample were transfected with pcDNA3.1 vector with no PhLP cDNA. (*B*) Similar experiments were performed with PhLP variants S25A and S296A separately and in combination with S18A/S19A/S20A. The data are also combined from three separate experiments. (*C*) The rate of nascent $G\beta_1\gamma_2$ dimer formation in the presence of CK2 phosphorylation site variants of PhLP was determined using a radiolabel pulse-chase assay. Time measurements indicate the sum of the 10-min pulse and the variable chase periods. A representative gel is shown. Band intensities were quantified, and molar ratios of $G\beta_1$ to HA-$G\gamma_2$ were calculated and plotted. *Lines* represent a fit of the data from three separate experiments to a first-order rate equation. Values for $t_{1/2}$ are shown next to the *graph*.

The manner in which PhLP binds CCT at the top of the apical domains without entering the folding cavity (Martin-Benito, Bertrand et al. 2004) suggests that PhLP, Gβ, and CCT might form a ternary complex in the process of Gβγ folding. If such a ternary complex does exist, then PhLP would be predicted to increase the binding of Gβ to CCT and *vice versa*. To test this possibility, the effects of PhLP or Gβ overexpression on the binding of the other to CCT was measured. As predicted, Gβ overexpression increased the binding of endogenous PhLP to CCT (Fig. 5*C*). However, PhLP overexpression unexpectedly caused a small but reproducible decrease in Gβ binding to CCT (Fig. 5*B*). It is possible that this decrease in Gβ binding to CCT might be caused by PhLP-catalyzed Gβγ assembly and release of the Gβγ dimer from CCT. To test this possibility, the effects of two PhLP variants that do not support Gβγ assembly on Gβ binding to CCT were also tested. One variant was PhLP S18A/S19A/S20A, and the other was a truncation variant in which residues 1–75 had been removed (PhLP Δ1–75) (Humrich, Bermel et al. 2005; Lukov, Hu et al. 2005). Both of these variants bind CCT, but they block Gβγ assembly in a dominant negative manner (Humrich, Bermel et al. 2005; Lukov, Hu et al. 2005). Overexpression of either of these variants increased endogenous Gβ binding to CCT dramatically (Fig. 5*B*). Thus, it appears that in the absence of serine 18–20 phosphorylation, PhLP forms a ternary complex with Gβ and CCT that cannot progress in the assembly process. It is interesting to note that the PhLP Δ1–75 variant binds Gβγ very poorly (Humrich, Bermel et al. 2005; Lukov, Hu et al. 2005), yet it is still able to stabilize the complex between Gβ and CCT. This observation indicates that PhLP Δ1–75 may do so, more through interactions with CCT than through interactions with Gβ.

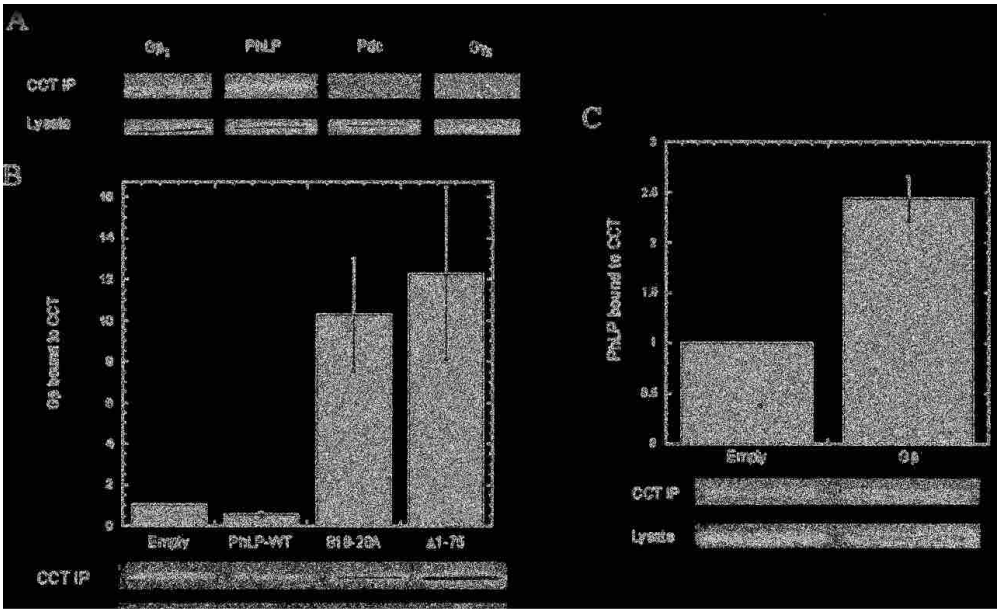

FIG. 3-5.Gβ binds CCT in a ternary complex with PhLP. (*A*) binding of Gβ to CCT was detected by co-immunoprecipitation. HEK-293 cells were transfected with FLAG-$G\beta_1$, PhLP, Pdc, or HA-$G\gamma_2$, and cell extracts were immunoprecipitated with an antibody to CCTε to bring down CCT complexes. The immunoprecipitates were immunoblotted for $G\beta_1$, PhLP, Pdc, or $G\gamma_2$. (*B*) The effects of PhLP on the binding of endogenously expressed Gβ to CCT were measured by co-immunoprecipitation. HEK-293 cells were transfected with wild-type PhLP, the PhLP S18A/S19A/S20A or Δ1-75 variants, or empty vector. Cell extracts were immunoprecipitated with the anti-CCTε antibody and immunoblotted for endogenous $G\beta_1$. A representative immunoblot is shown. *Bars* in the *graph* represent the average ± standard error of the Gβ band intensity relative to the empty vector control from four separate experiments. (*C*) The effects of Gβ on the binding of endogenously expressed PhLP to CCT were also measured by co-immunoprecipitation. HEK-293 cells were transfected with $G\beta_1$, CCT was immunoprecipitated as in *panel B*, and samples were immunoblotted for endogenous PhLP. A representative immunoblot is shown. *Bars* in the *graph* represent the average ± standard error of the PhLP band intensity relative to the empty vector control from three separate experiments.

PhLP phosphorylation is required for the release of Gβ from CCT and interaction with Gγ–To further investigate the apparent correlation between the destabilization of the PhLP·Gβ·CCT ternary complex by PhLP phosphorylation and the requirement for PhLP phosphorylation in Gβγ assembly, the effects of Gγ on ternary complex formation with several PhLP variants was measured. This work was performed by Georgi Lukov and

Christine Baker, and is included for the purpose of completeness. Gβ was overexpressed in HEK-293 cells with Gγ and PhLP variants as indicated, and the amount of Gβ co-immunoprecipitating with CCT was measured (Fig. 6*A*). Co-expression of Gγ caused a decrease in Gβ binding to CCT that was intensified by the co-expression of wild-type PhLP. In striking contrast, Gβ binding to CCT was greatly enhanced by co-expression of PhLP Δ1-75 and was completely insensitive to co-expression of Gγ. Co-expression of PhLP S18A/S19A/S20A also enhanced Gβ binding to CCT significantly, and Gγ had much less of an effect on binding than with wild-type PhLP. Interestingly, the effects of PhLP Δ1-75 and S18A/S19A/S20A on Gβ binding to CCT in the presence of Gγ were quantitatively very similar to their effects on Gβγ assembly. PhLP Δ1-75 completely blocked Gβγ assembly (Humrich, Bermel et al. 2005; Lukov, Hu et al. 2005) and Gγ-mediated dissociation of Gβ from CCT, whereas PhLP S18A/S19A/S20A decreased the rate of Gβγ assembly by 15-fold (Humrich, Bermel et al. 2005; Lukov, Hu et al. 2005) and Gγ-induced dissociation of Gβ from CCT by 9-fold (compare the Gβγ PhLP-WT sample to the Gβγ PhLP S18A/S19A/S20A sample in Fig. 6*A*). From these data, it appears that PhLP phosphorylation contributes to Gβγ assembly by enhancing the ability of Gγ to release Gβ from the ternary complex.

There are two possible mechanisms by which phosphorylated PhLP could contribute to Gγ-mediated release of Gβ from CCT. Both involve a conformational change in the ternary complex upon PhLP phosphorylation. First, PhLP phosphorylation could induce a conformation that allows Gγ to access Gβ in the ternary complex and form the Gβγ dimer. The Gβγ would then be released from CCT. Second, phosphorylation could induce

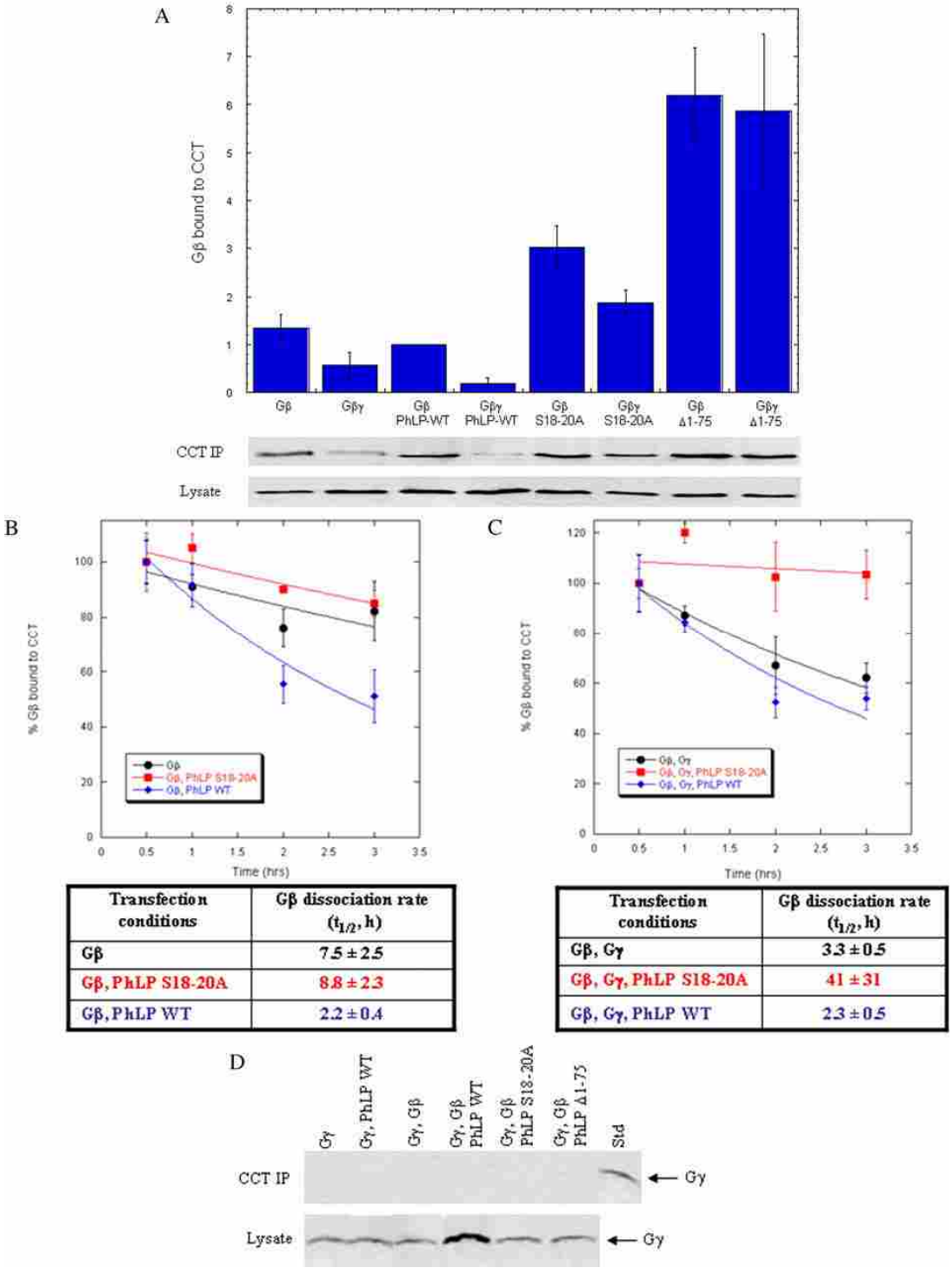

Transfection conditions	Gβ dissociation rate ($t_{1/2}$, h)
Gβ	7.5 ± 2.5
Gβ, PhLP S18-20A	8.8 ± 2.3
Gβ, PhLP WT	2.2 ± 0.4

Transfection conditions	Gβ dissociation rate ($t_{1/2}$, h)
Gβ, Gγ	3.3 ± 0.5
Gβ, Gγ, PhLP S18-20A	41 ± 31
Gβ, Gγ, PhLP WT	2.3 ± 0.5

FIG. 3-6.PhLP phosphorylation is required for the release of Gβ from CCT and interaction with Gγ. (*A*), the effects of PhLP phosphorylation and Gγ co-expression on Gβ binding to CCT were measured by co-immunoprecipitation. HEK-293 cells were transfected with FLAG-$G\beta_1$, HA-$G\gamma_2$, and the PhLP variants as indicated. Cell extracts were immunoprecipitated with an antibody to CCTε and then immunoblotted for FLAG-Gβ. A representative immunoblot is shown. *Bars* in the *graph* represent the average ± S.E. of the Gβ band intensity relative to the Gβ/PhLP-WT sample from three separate experiments. (*B*), the effects of PhLP phosphorylation on the rate of Gβ release from CCT were measured using a radiolabel pulse-chase assay. HEK-293 cells were transfected with FLAG-$G\beta_1$ and the indicated PhLP variants. The pulse-chase assay was performed as in Fig. 4*C*. After the chase times indicated, cell extracts were immunoprecipitated with antibodies to CCTε or $G\beta_1$. Proteins were resolved by SDS-PAGE, and radiolabeled bands were detected using a Phosphorimager. The Gβ band intensities were quantified, and ratios of nascent $G\beta_1$ in the CCT immunoprecipitate *versus* the total nascent Gβ in the Gβ immunoprecipitate were calculated and plotted as a percentage of the ratio at the first time point. *Lines* represent a fit of the data from 3 separate experiments to a first-order rate equation. Values for $t_{1/2}$ are shown *below* the *graph.* (*C*), the effects of Gγ on PhLP-mediated release of nascent $G\beta_1$ from CCT were measured as in *panel B* in HEK-293 cells co-expressing HA-$G\gamma_2$ in addition to FLAG-$G\beta_1$ and PhLP. (*D*), the ability of Gγ to bind CCT was assessed by co-immunoprecipitation. HEK-293 cells were transfected with FLAG-$G\beta_1$, HA-$G\gamma_2$, or PhLP variants as indicated. Cells extracts were immunoprecipitated with an antibody to CCTε and then immunoblotted for Gγ.A representative blot is shown. The *Std lane* in the *CCT IP panel* was the lysate from the Gγ-transfected cells.

a conformation that releases PhLP·Gβ from CCT, thereby freeing the Gγ binding site on Gβ for Gβγ association to occur. To distinguish between these two mechanisms, the effects of Gγ and PhLP overexpression on the rate of dissociation of Gβ from CCT were measured. In this experiment, cells co-expressing Gβ with Gγ, PhLP, or PhLP S18A/S19A/S20A were pulsed with [^{35}S]methionine for 10 min to label the nascent polypeptides and then were chased with unlabeled methionine. At the times indicated, the cells were lysed and CCT was immunoprecipitated. The co-immunoprecipitating proteins were separated by SDS-PAGE, and the amount of ^{35}S in the Gβ band was quantified. In the absence of PhLP or Gγ co-expression, the dissociation rate of nascent Gβ from CCT was very slow, with a $t_{1/2}$ of ~8 h. PhLP co-expression increased the rate by 4-fold to a $t_{1/2}$ of ~2 h. In contrast, PhLP S18A/S19A/S20A co-expression did not increase the dissociation rate (Fig. 6*B*). When Gγ was co-expressed with Gβ, the dissociation rate

increased by >2-fold to a $t_{1/2}$ of ~3 h, whereas, when both Gγ and PhLP were co-expressed, the $t_{1/2}$ increased even further to ~2 h, the same value observed in the absence of Gγ overexpression (Fig. 6*C*). When PhLP S18A/S19A/S20A was co-expressed with Gγ, there was essentially no Gβ dissociation, similar to what was seen in the absence of Gγ overexpression (Fig. 6*C*). These effects of Gγ, PhLP, and PhLP S18A/S19A/S20A on the dissociation rates are consistent with their effect on the steady-state binding of Gβ to CCT (Fig. 6*A*) and further demonstrate that PhLP phosphorylation is required for the release of Gβ from the ternary complex.

These findings are able to distinguish between the two potential mechanisms mentioned above. For example, the enhanced rate of dissociation of Gβ from CCT upon PhLP overexpression in the absence of Gγ overexpression (Fig. 6*B*) is consistent with the second mechanism in which a phosphorylated PhLP·Gβ complex would be released prior to Gγ binding to Gβ. This result would not be expected in the first mechanism in which Gγ binding would be required for release of Gβ from CCT. Similarly, the observed lack of increase in the Gβ dissociation rate upon co-expression of Gγ with PhLP would be predicted by the second mechanism but not by the first. On the other hand, the increased release of Gβ from CCT upon Gγ overexpression in the absence of PhLP overexpression is consistent with the first mechanism, but this result could also be explained by the second mechanism if the endogenous PhLP were acting catalytically to release Gβ from CCT for association with Gγ. In this case, the dissociation process would be drawn forward by the formation of the Gβγ dimer and its association with Gα and cell membranes (Fig. 7). To further assess the role of Gγ in the release of Gβ from CCT, the

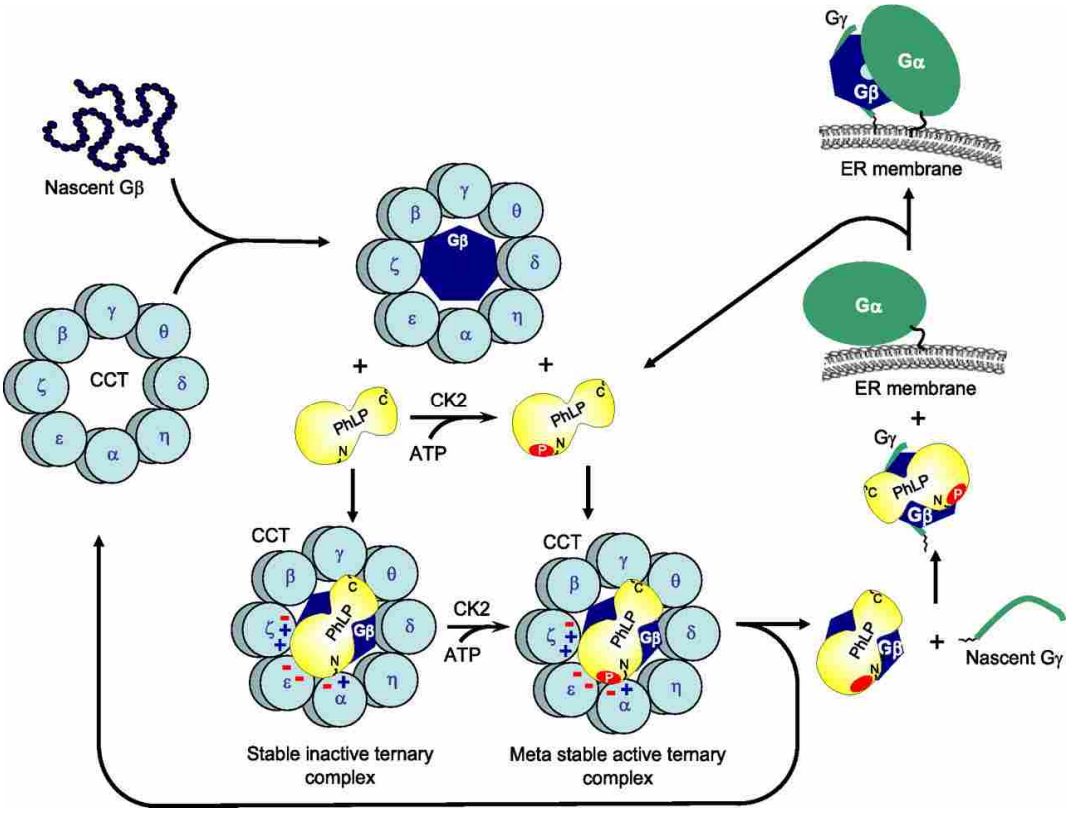

FIG. 3-7.CK2 phosphorylation-dependent release model of Gβγ assembly. A model is proposed in which nascent Gβ forms a ternary complex with CCT and PhLP. If PhLP is not phosphorylated, the ternary complex is stable and PhLP·Gβ is not released from CCT. If PhLP is phosphorylated, the ternary complex is destabilized, possibly by electrostatic repulsion between the phosphates in the serine 18–20 phosphorylation site and negatively charged residues on the CCTα or -ε apical domains. Once released, the PhLP·Gβ complex binds Gγ, forming the Gβγ dimer. The dimer then associates with Gα and membranes in a manner yet to be defined. In the process, PhLP is released to catalyze another round of dimer formation. The approximate position of the serine 18–20 phosphorylation site is depicted by a *red oval* marked `*P*.' The relative amount of positive and negative charges on the CCT apical domains that contact the PhLP N-terminal domain is also indicated.

possible association of Gγ with Gβ and PhLP in CCT complexes was determined. Gγ was co-expressed with the indicated combinations of Gβ and the PhLP variants, the CCT complexes were immunoprecipitated, and the samples were immunoblotted for Gγ. Gγ was not found in any of the CCT immunoprecipitates (Fig. 6*D*), despite the fact that Gβ and PhLP could be readily found under these conditions (see Fig. 5). Thus, it appears that

Gγ does not interact with CCT in any of its complexes with Gβ and PhLP. Together, the data in Fig. 6 indicate that PhLP phosphorylation results in the release of a PhLP·Gβ complex from CCT that can then associate with Gγ to form the Gβγ dimer. This conclusion is also supported by the previously reported observation that PhLP forms a stable complex with Gβ that does not include Gγ (Lukov, Hu et al. 2005).

DISCUSSION

A model for Gβγ assembly–Recent studies have shown that PhLP acts as an essential chaperone in the assembly of Gβγ dimers by binding the Gβ subunit and thereby allowing Gγ to associate with Gβ (Humrich, Bermel et al. 2005; Lukov, Hu et al. 2005). Phosphorylation of PhLP at serines 18–20 by CK2 was required for Gβγ assembly to occur, yet the means by which phosphorylation of serines 18-20 contributes to assembly was unknown. Moreover, CCT had been implicated in the assembly process, but the results were conflicting (Martin-Benito, Bertrand et al. 2004; Humrich, Bermel et al. 2005; Lukov, Hu et al. 2005). The current study provides evidence for a molecular mechanism describing both the role of CCT and PhLP phosphorylation in Gβγ assembly (Fig. 7). There are five important steps in this mechanism: 1) the nascent Gβ polypeptide binds CCT. This is a stable complex that releases Gβ very slowly in the absence of PhLP. 2) PhLP binds forming a ternary complex. If PhLP is not phosphorylated, then the ternary complex forms in a stable conformation that does not release PhLP·Gβ, and the Gβγ assembly process is blocked. However, if PhLP is dually phosphorylated within the serine

18–20 sequence, then the ternary complex assembles in a conformation that readily releases the PhLP·Gβ dimer. 3) PhLP·Gβ dissociates from CCT. The structure of the Pdc·G_{τ}βγ complex shows that Pdc binds Gβ on the opposite face as Gγ (Gaudet, Bohm et al. 1996), predicting that the Gγ binding site on Gβ would be free in the PhLP·Gβ dimer. 4) Gγ binds Gβ forming a PhLP·Gβγ complex. This complex is stable with a 100 nM binding affinity (Savage, McLaughlin et al. 2000). However, both the Gα binding site and the membrane association surface of Gβγ overlap extensively with the PhLP binding site (Savage, McLaughlin et al. 2000); therefore in the presence of Gα and membranes, PhLP would be expected to be released from Gβγ. 5) Gβγ associates with Gα and/or the endoplasmic reticulum membrane and is transported to the plasma membrane (Michaelson, Ahearn et al. 2002). PhLP is then free to catalyze another round of Gβγ assembly.

This model readily explains the dominant negative effect of the PhLP S18A/S19A/S20A and PhLP Δ1-75 variants. These variants form PhLP·Gβ·CCT ternary complexes that do not release PhLP·Gβ for Gγ binding. Such stable ternary complexes would also block the endogenous, phosphorylated PhLP from forming competent ternary complexes capable of releasing PhLP·Gβ for Gγ binding. Previous explanations of the dominant negative effect of PhLP S18A/S19A/S20A, which postulated that unphosphorylated PhLP would block Gβ and Gγ association with CCT (Humrich, Bermel et al. 2005) or that unphosphorylated PhLP would form a PhLP·Gβ complex that would not accept Gγ (Lukov, Hu et al. 2005), are incomplete.

Phosphorylation-induced conformational changes—One apparent inconsistency in the data is that CK2 phosphorylation of PhLP increased its binding to CCT in the absence of Gβ (Fig. 1), yet PhLP phosphorylation was necessary for the release of PhLP·Gγ from CCT in the presence of Gβ (Figs. 4, 5, and 6). The difference between these observations may stem from differences in the structures of the PhLP·CCT and PhLP·Gβ·CCT complexes. Clues regarding the nature of the phosphorylation-dependent changes in these structures may be gleaned from the cryoelectron microscopic studies of the unphosphorylated PhLP·CCT complex (Martin-Benito, Bertrand et al. 2004). In this complex, PhLP was shown to interact in two distinct conformations at the top of the CCT toroid, contacting only the CCT apical domains (Martin-Benito, Bertrand et al. 2004). In one conformation, the N-terminal phosphorylation site of PhLP was in close proximity to the CCTα and -ε apical domains and in the other conformation the phosphorylation site was in close proximity to the CCTζ and -β apical domains. The binding surfaces of all eight apical domains are dominated by charged and polar residues (Pappenberger, Wilsher et al. 2002) with the CCTα and -ε binding surfaces having a high distribution of negative charge, whereas the CCTζ binding surface exhibits an extensive positively charged patch. The serine 18–20 phosphorylation site of PhLP is harbored within a sequence (^{18}SSSDEDESD^{26}) that is already very negatively charged. The addition of phosphates within this sequence would create an extremely high concentration of negative charge that would interact effectively with the positively charged patch of CCTζ. In the absence of Gβ, phosphorylation could favor the conformation that brings the PhLP phosphorylation site in close proximity to the CCTζ apical domain, increasing the binding of PhLP to CCT. In the presence of Gβ, it is possible that interactions with Gβ

may limit the ability of PhLP to rotate on the top of the CCT toroid. Thus, the phosphorylation site may be fixed in close proximity to the CCTα and -ε apical domains, causing electrostatic repulsion between the negative charges on the CCTα and -ε binding surfaces and the PhLP phosphorylation site. This repulsion might destabilize the ternary complex and allow the release of the PhLP·Gβ complex. Further studies will be required to test the validity of this structural model.

Regulation of CK2 Phosphorylation of PhLP–Given the essential role of CK2 phosphorylation of PhLP in Gβγ dimer formation, an important issue yet to be addressed is the regulation of this phosphorylation event. CK2 is a constitutively active kinase with many protein substrates (Litchfield 2003). Determination of which substrates are phosphorylated and when phosphorylation occurs appears to be controlled by regulated expression and assembly of the CK2 $\alpha_2\beta_2$ tetramer and by the association of different CK2 binding partners (Litchfield 2003). In the case of PhLP, CK2 phosphorylation occurs within the first 30 min of its synthesis (data not shown), and it remains completely phosphorylated under the cell culture conditions used here (Fig. 2). It is not clear from the current data whether phosphorylation occurs prior to or after association of PhLP with CCT (Fig. 7). In mouse tissues, PhLP was also completely phosphorylated in brain and heart but was mostly unphosphorylated in the adrenal gland (Humrich, Bermel et al. 2003). It is possible that Gβγ assembly is a continuous process in some cell types, whereas in others assembly is highly regulated, only occurring under certain conditions that promote CK2 phosphorylation of PhLP.

These investigations into the mechanism of PhLP-mediated Gβγ assembly and its regulation by CK2 phosphorylation suggest that PhLP and its interactions with Gβ and CCT could be targeted by therapeutics to control the levels of Gβγ expression and thus the degree of G protein signaling within the cell, perhaps providing additional tools to treat the myriad of G protein-linked diseases.

CHAPTER 4

PURIFICATION OF THE G PROTEIN β SUBUNIT, PHOSDUCIN-LIKE PROTEIN, AND THE CYTOSOLIC CHAPERONIN TERNARY COMPLEX

Introduction–Initial reports describing the interaction between PhLP and its binding partners CCT and Gβγ postulated the role of PhLP may be to regulate G protein signaling by sequestering Gβγ from Gα and its effectors, or conversely that CCT may regulate G protein signaling by sequestering PhLP (Bauer, Muller et al. 1992; Lee, Ting et al. 1992; Hawes, Touhara et al. 1994; Gaudet, Bohm et al. 1996). This role of PhLP as a negative regulator of G protein signaling followed well the role of Phosducin (Pdc), which has been reported to act as a negative regulator of G protein signaling by sequestering the G protein βγ subunit from the outer segment in light-activated photoreceptor rod cells (Sokolov, Strissel et al. 2004). However, initial reports on the role of PhLP as a negative regulator were inconclusive and the significance of its interactions with its binding partners initially remained elusive. In addition, several inconsistencies arose in the sequestration model. First, expression levels of PhLP were reported to be significantly lower than that of Gβγ (Schroder and Lohse 2000) and most data showing down regulation of G protein signaling required significant overexpression of PhLP, raising doubts about the ability of PhLP to sequester enough Gβγ in order to have an effect on G protein signaling under physiological conditions. Second, evidence suggested PhLP to be constitutively bound to Gβγ with no apparent mechanism of regulation (Thulin, Howes et

al. 1999). Third, strong evidence suggesting the role of PhLP as a positive regulator of G protein signaling came from two separate studies showing that deletion of the *PhLP1* gene in chestnut blight fungus *Cryphonectria parasitica* (Kasahara, Wang et al. 2000) and in *Dictyostelium discoideum* (Blaauw, Knol et al. 2003) abolished G protein signaling and yielded the same phenotype as deletion of the Gβ gene.

Further insight into the role of PhLP emerged from structural and biochemical studies of PhLP bound to CCT. The structure of the PhLP·CCT complex obtained from cryo electron microscopy studies showed that PhLP sits above the CCT folding cavity, contacting the apical domains of the CCT subunits and occluding the entrance into the cavity similar to that of prefoldin, a co-chaperonin required for actin and tubulin folding (Martin-Benito, Bertrand et al. 2004). In addition it has been shown that PhLP does not bind CCT as a folding substrate, but rather binds CCT in its native form, suggesting a regulatory role for PhLP as a co-chaperonin (McLaughlin, Thulin et al. 2002).

The strongest evidence so far for the role of PhLP comes from data which shows that PhLP is an essential chaperone in the formation of the Gβγ dimer (Lukov, Hu et al. 2005). In this report, it was shown that $G\beta_1$ expression dropped 40% without affecting $G\beta_1$ mRNA levels when PhLP1 expression was inhibited using RNA interference. In addition, PhLP1 depletion inhibited histamine-mediated increases in cytosolic Ca^{2+} via Gq by 60%. This reduction in $G\beta_1$ expression and G protein signaling suggests a critical role for PhLP in the formation of the Gβγ dimer.

The most recent findings show that PhLP forms a ternary complex with Gβ and CCT and that phosphorylation of PhLP within the S18–20 sequence is required for the release of

Gβ from CCT (Lukov, Baker et al. 2006). Furthermore, it was shown that the rate of release of Gβ from CCT was not increased by overexpressing Gγ, suggesting that the PhLP·Gβ complex dissociates from CCT prior to Gγ binding to Gβ to form the Gβγ complex. In addition, it has been shown that Gβ binds CCT prior to its interaction with Gγ and that the ATPase cycle of CCT was necessary for Gβ release, enabling its association with Gγ (Wells, Dingus et al. 2006).

Together these data suggest an important role for PhLP in Gβγ dimer assembly. In order to better understand the mechanism of Gβγ dimer assembly and the role of phosphorylation within the S18–20 sequence of PhLP, the PhLP·Gβ·CCT ternary complex was expressed and purified from insect cells for x-ray crystallographic and cryo electron microscopy structural studies.

EXPERIMENTAL PROCEDURES

Construction of recombinant transfer vector for PhLP-TEV-myc-His–The cDNA for the wild-type human PhLP with a 3´ c-myc and His_6 tag was previously constructed in the pcDNA 3.1/myc-His B vector (Lukov, Hu et al. 2005). A pBlueBac4.5 vector encoding a C-terminal TEV protease cleavable myc-His_6 tag was constructed by introducing the TEV protease site into the cDNA using PCR. The T7-forward primer site of pcDNA3.1 was used with a reverse primer encoding an *Xba*I restriction site (underlined), with the 7 amino acids of the TEV protease site (ENLYFQG) and the C-terminal sequence of human PhLP (5´-CCG CGG GCC C<u>TC TAG A</u>CC CTG AAA ATA CAA ATT CTC

ATC TAT TTC CAG GTC GCT ATC CTC-3´). The expected 1,025-bp of PCR product was purified on 1% TE agarose gel and digested with *Eco*RI and *Xba*I. The expected 929 bp DNA fragment was purified and cloned into *Eco*RI/*Xba*I sites of pcDNA3.1 vector and its sequence was confirmed. The open reading frame of PhLP-TEV-myc-His was PCR amplified using the T7-forward primer and BGH reverse primer sites of pcDNA3.1/myc-His B vector. The expected 1,131-bp PCR product was purified on 1% TE agarose gel and digested with *Bam*HI and *Age*I. The expected 1,006-bp fragment was purified and cloned into *Bam*HI/*Age*I sites of pBlueBac4.5 vector and its sequence was confirmed.

Construction of recombinant transfer vector for Gβ_1-HPC4–A pBlueBac4.5 vector encoding C-terminal HPC4 epitope-tagged Gβ_1 was constructed by introducing the HPC4 epitope into the cDNA using PCR. The cDNA for the wild-type human Gβ_1 in the pcDNA3.1 vector was obtained from the University of Missouri-Rolla cDNA Resource Center. The T7-forward primer was used with a reverse primer encoding an *Xba*I restriction site (underlined), the 12 amino acids of the HPC4 epitope (EDQVDPRLIDGK) and the C-terminal sequence of human Gβ_1, (5´-CGT AC<u>T CTA GA</u>T TAC TTG CCG TCG ATC AGC CTG GGG TCC ACC TGG TCC TCG TTC CAG ATC TTG AGG AAG CTA TCC CAG G-3´). The expected 3,255-bp of PCR product was purified on a 0.7% TE agarose gel and digested with *Bam*HI and *Xba*I. The expected 3,191-bp DNA fragment was purified and cloned into the *Bam*HI/*Xba*I sites of pBlueBac4.5 vector and its sequence was confirmed.

Production of recombinant baculoviruses containing PhLP-TEV-myc-His and Gβ$_1$-HPC4–pBlueBac4.5- PhLP-TEV-myc-His and pBlueBac4.5- Gβ$_1$-HPC4 constructs were co-transfected with linearized Bac-N-Blue™ viral DNA (AcMNPV, *Autographa californica* multiple nuclear polyhedrosis virus) in the presence of Cellfectin™ reagent insect cell-specific liposomes, into *Spodoptera frugiperda* (*Sf*9) insect cells (Invitrogen). The recombinant baculovirus was identified and purified by plaque assay and the putative recombinant plaques were transferred to 12-well microtiter plates and amplified in *sf*9 cells. Viral DNA was purified for PCR analysis to determine the purity of recombinant viruses. High titer viral stocks were generated by amplification in *sf*9 cell suspension cultures according to the manufacturer's instructions.

Expression of PhLP-TEV-myc-His and Gβ$_1$-HPC4 in insect cells–High Five™ cells (Invitrogen) were cultured at 27°C in EX-CELL™ 405 serum-free medium (SAFC Biosciences) supplemented with 100 units of penicillin-streptomycin/ml (Gibco) in culture spinner flasks with constant stirring at 80 rev/min. When the cell density reached 2 X 10^6 cells/ml, they were inoculated with high titer viral stocks of the PhLP-TEV-myc-His and G protein β$_1$-HPC4 expressing recombinant baculoviruses at a multiplicity of infection of 15 viral particles per cell.

Purification of complexes containing PhLP, Gβ$_1$, and CCT–All purification steps were conducted at 4°C with ice-cold buffers supplemented with 1 mM phenylmethylsulfonyl fluoride. Cells were harvested 84 hours after baculovirus inoculation by adding 1:20 Insect PopCulture™ (Novagen) lysis reagent to the cell culture and stirring for 20 minutes. Lysate was centrifuged at 3,500g for 10 min, after which the supernatant was

treated with 25KU of Benzonase Nuclease HC (Novagen)/150ml supernatant and dialyzed overnight in dialysis buffer (20 mM HEPES, pH 8.0, 20mM NaCl, and 2mM $MgCl_2$, 0.05% CHAPS). Following dialysis, the lysate was loaded onto a Ni-NTA agarose (Invitrogen) column, washed with 4 column volumes of dialysis buffer, and the complex eluted with Ni-NTA elution buffer (20 mM HEPES, pH 7.0, 150 mM NaCl, 500 mM imidazole, 0.05% CHAPS). The elutant off the Ni-NTA column was supplemented with 2 mM Ca^{2+} and then loaded onto an HPC4 affinity agarose (Roche Applied Sciences) column equilibrated with equilibration buffer (20 mM HEPES, pH 7.5, 250 mM $NaCl_2$, 2 mM $CaCl_2$). The column was washed with HPC4 equilibration buffer, and the complex was eluted with HPC4 elution buffer (20 mM HEPES, pH 7.5, 500 mM NaCl, 10 mM EDTA, 0.05% CHAPS).

Analysis of the purified ternary complex by SDS-PAGE and immunoblotting–To determine the purity of the HPC4 eluant and to confirm the presence of PhLP and $G\beta_1$, 15 µl of eluant off the HPC4 affinity column was electrophoresed on an SDS/PAGE gel (10%) with 5 µl of 4X Laemmli sample buffer and either Coomassie stained or transferred to nitrocellulose membrane for immunoblotting. Membranes were immunoblotted with rabbit antiserum against the N-terminal 50 amino acids of PhLP and the N-terminal 15 amino acids of $G\beta_1$. Dilutions for primary antibodies were as follows: anti PhLP, 1:5,000; anti-$G\beta_1$, 1:2,500. The blots were incubated in goat anti-rabbit secondary antibody at a dilution of 1:10,000 for 1 hr at 4°C and developed using an Odyssey infrared imaging system (LI-COR Biosciences, Lincoln, NE).

Mass spectrometric analysis of purified $G\beta_1$, PhLP, and CCT ternary complex– In order to confirm the identity of the individual bands and the existence of CCT in the eluant, gel bands were excised and identified using electrospray tandem mass spectrometry (LCMSMS). Fifteen microliters of elutant off the HPC4 affinity column was electrophoresed on an SDS/PAGE gel (10%) with 5 µl of 4X Laemmli sample buffer and Coomassie stained. Bands were excised, in-gel digested as described previously (Shevchenko, Wilm et al. 1996), and injected onto a C18 reversed-phase resin capillary column and eluted using a gradient of 5 to 95% acetonitrile in 0.1% formic acid. Fragmentation spectra were analyzed using BioAnalyst software (Applied Biosystems, Farmingham, MA). Collision induced dissociation (CID) spectra for the three most intense ions from each scan were selectively chosen and submitted to the Mascot (Matrix Science) website for peptide identification.

RESULTS

Purification of the PhLP·$G\beta_1$·CCT ternary complex– High Five ™ insect cells (Invitrogen) were inoculated with high titer viral stock of PhLP-TEV-myc-His and $G\beta_1$-HPC4-expressing recombinant baculovirus. PhLP·$G\beta_1$·CCT ternary complexes from the cell culture were purified using Ni^{2+} affinity chromatography followed by further purification with an immobilized HPC4 antibody column as described in *Experimental Procedures*. A Coomassie-stained gel of the purified product revealed bands at ~38kDa and ~45kDa along with a cluster of bands around ~60–65kDa, which correspond to the molecular weights of $G\beta_1$, PhLP, and CCT subunits respectively (Fig 1). The 38 kDa

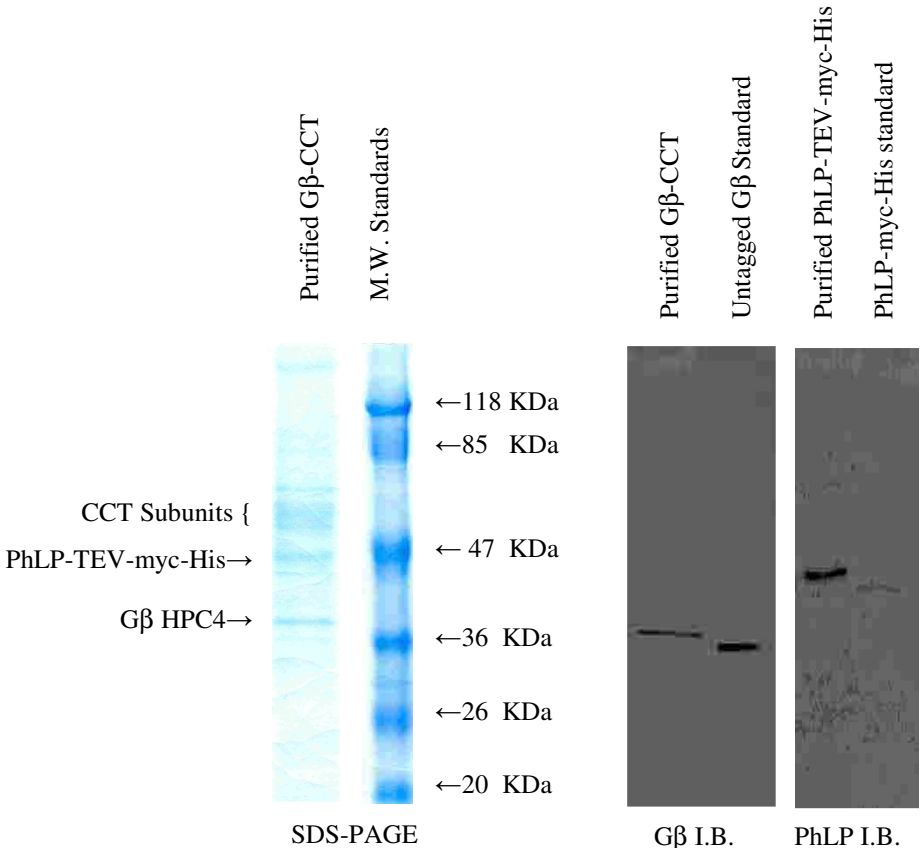

Fig. 4-1. Purufication of the Gβ·CCT·PhLP complex. The SDS-PAGE gel shows the HPC4-tagged Gβ, PhLP, and a cluster of CCT bands. Immunoblots confirm the identity of the PhLP and Gβ bands.

band was recognized by a $G\beta_1$ antibody and the 45 kDa band was recognized by a PhLP antibody in immunoblots (Fig. 1). No antibodies were available against insect cell CCT subunits and therefore mass spectrometry was used to identify the 60-65 kDa cluster of bands. Gel bands were excised, in-gel digested with trypsin and prepared for mass spec analysis. Good quality CID spectra (defined as spectra with a P value<0.05) for six of the seven bands were obtained, while sample from band #5 did not yield credible protein

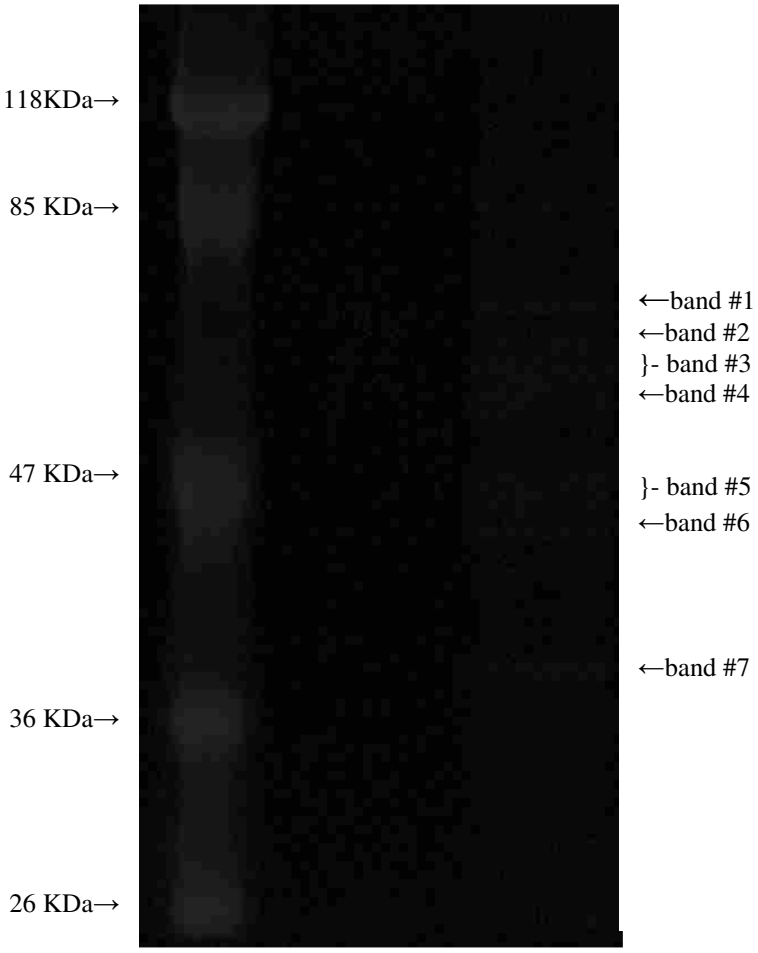

Fig. 4-2. Mass spectrometric identification of proteins in the purified complex. The product off the HPC4 column was analyzed by SDS-PAGE and the gel bands were excised and in-gel digested with trypsin. The cleaved peptides were then analyzed by LCMSMS and their parent proteins were identified by searching the NCBI non-redundant protein database using the Mascot program. The table gives the identity of the bands. Numeric values indicate the probability score for a given identification with higher scores indicating greater confidence. Generally probability scores in the 30-40 range gave $p < 0.05$, and all of these identifications were well within the $p < 0.05$ limit.

Band	Identity	Mascot score
1	Albumin	200
2	CCTζ, CCTγ	169, 87
3	CCTα, CCTβ	134, 153
4	CCTη	55
5	No I.D.	
6	PhLP1	68
7	$G\beta_1$	144

identification. Band #1 was identified as albumin (Fig. 2.). Bands 2, 3 and 4 were identified as CCT bands with band 2 containing CCT subunits ζ and γ, band 3 containing CCT α and β, and band 4 containing the CCT η. Bands 6 and 7 were identified as human PhLP and Human $G\beta_1$. The Mascot scores for each band are shown in Fig. 2. These results indicate that a complex between CCT, PhLP and $G\beta_1$ was purified with only minor impurities. Final yields of the complex were typically in the range of 500-900 μg of total protein from 500 ml of cell culture.

DISCUSSION

Recently published data show that PhLP forms a ternary complex with Gβ and CCT in the process of Gβγ assembly and that phosphorylation of PhLP within the S18–20 sequence is necessary for the release of a PhLP-Gβ intermediate from CCT for association of Gβ with Gγ (Lukov et al. 2006). In order to understand the structural mechanism by which phosphorylation of PhLP destabilizes the PhLP·Gβ·CCT ternary complex, we have purified the complex for cryo-electron microscopic and x-ray crystallographic structural studies. We have shown that it is possible to obtain sufficient quantities of the complex for cryo electron microscopy (~ 100 μg protein). However, in order to begin X-ray crystallography studies, a higher quantity of sample (>5 mg protein) and an additional purification step such as gel-filtration will be required. In order to obtain higher yields, scale-up of the purification will be necessary. The efficiency of the purification suggests that simply increasing the volume of insect cell culture and the size of the affinity columns may be sufficient to obtain the necessary yields.

The results of this purification further confirm previous data suggesting the existence of a ternary complex between PhLP, Gβ, and CCT. Now that the ternary complex is isolated, the cryo-EM and X-ray crystallographic structural determinations can proceed in earnest. By comparing the structures of the ternary in both states of PhLP phosphorylation, the mechanism by which S18-20 phosphorylation triggers the release of PhLP-Gβ will be revealed. In addition, X-ray determinations will show the atomic structure of the CCT complex for the first time, elucidating the ways in which this multi-subunit complex functions so elegantly to catalyze the folding of its protein substrates. Previous attempts to crystallize CCT have been unsuccessful, probably because of the flexibility of the apical domains. The formation of the PhLP-Gβ-CCT complex will decrease this flexibility as a result of the contacts between PhLP and the CCT apical domains and should increase the chances of obtaining stable crystals significantly. Determination of the structure of the PhLP-Gβ-CCT complex would represent a major breakthrough in the understanding of protein folding by CCT and the co-chaperoning role of PhLP in this process.

REFERENCES

Aloy, P., B. Böttcher, et al. (2004). "A novel step in beta-tubulin folding is important for heterodimer formation in Saccharomyces cerevisi." Science **165**: 531-541.

Bauer, P. H., S. Muller, et al. (1992). "Phosducin is a protein kinase A-regulated G-protein regulator." Nature **358**: 73-76.

Blaauw, M., J. C. Knol, et al. (2003). "Phosducin-like proteins in Dictyostelium discoideum: implications for the phosducin family of proteins. ." Embo J **22**: 5047-5057.

Bootman, M., E. Niggli, et al. (1997). "Imaging the hierarchical Ca2+ signalling system in HeLa cells." J Physiol **499 (Pt 2)**: 307-14.

Braig, K., Z. Otwinowski, et al. (1994). "The crystal structure of the bacterial chaperonin GroEL at 2.8 A." Nature **371**(6498): 578-86.

Cabrera-Vera, T. M., J. Vanhauwe, et al. (2003). "Insights into G protein structure, function, and regulation." Endocr Rev **24**(6): 765-81.

Camasses, A., A. Bogdanova, et al. (2003). "The CCT chaperonin promotes activation of the anaphase-promoting complex through the generation of functional Cdc20." Mol Cell **12**(1): 87-100.

Carter, M. D., K. Southwick, et al. (2004). "Identification of phosphorylation sites on phosducin-like protein by QTOF mass spectrometry." J Biomol Tech **15**(4): 257-64.

Choquet, Y., K. Wostrikoff, et al. (2001). "Assembly-controlled regulation of chloroplast gene translation." Biochem Soc Trans **29**(Pt 4): 421-6.

Clapham, D. E. and E. J. Neer (1993). "New roles for G-protein beta-gamma dimmers in transmembrane signaling " Nature **365**: 403-406.

Clapham, D. E. and E. J. Neer (1997). "G protein beta/gamma subunits." Annu Rev Biochem **37**: 167-203.

Ditzel, L., J. Lowe, et al. (1998). "Crystal structure of the thermosome, the archaeal chaperonin and homolog of CCT." Cell **93**(1): 125-38.

Elbashir, S. M., J. Harborth, et al. (2001). "Duplexes of 21-nucleotide RNAs mediate RNA interference in cultured mammalian cells." Nature **411**(6836): 494-8.

Ellis, R.J., (1996) in *The Chaperonins*, ed. Ellis, R.J. (Academic, San Diego), pp. 2–25.

Ellis, R. J. and F. U. Hartl (1999). "Principles of protein folding in the cellular environment." Curr Opin Struct Biol **9**(1): 102-10.

Flanary, P. L., P. R. DiBello, et al. (2000). "Functional analysis of Plp1 and Plp2, two homologues of phosducin in yeast." J Biol Chem **275**(24): 18462-9.

Ford, C. E., N. P. Skiba, et al. (1998). "Molecular basis for interactions of G protein betagamma subunits with effectors." Science **280**: 1271-1274.

Frank, J. (1996). Three-Dimensional Electron Microscopy of Macromolecular Assemblies.

Gainetdinov, R. R., R. T. Premont, et al. (2004). "Desensitization of G protein-coupled receptors and neuronal functions." Annu Rev Neurosci **27**: 107-44.

García-Higuera, I., C. Gaitatzes, et al. (1998). "Folding a WD repeat propeller. Role of highly conserved aspartic acid residues in the G protein beta subunit and Sec13. ." J Biol Chem **273**: 9041-9049.

Garzon, J., M. Rodriguez-Diaz, et al. (2002). "Glycosylated phosducin-like protein long regulates opioid receptor function in mouse brain." Neuropharmacology **42**(6): 813-28.
Gaudet, R., A. Bohm, et al. (1996). "Crystal structure at 2.4 angstroms resolution of the complex of transducin betagamma and its regulator, phosducin." Cell **87**(3): 577-88.
Gaudet, R., J. R. Savage, et al. (1999). "A molecular mechanism for the phosphorylation-dependent regulation of heterotrimeric G proteins by phosducin." Mol Cell **3**(5): 649-60.
Gensse, M., N. Vitale, et al. (2000). "Regulation of exocytosis in chromaffin cells by phosducin-like protein, a protein interacting with G protein betagamma subunits." FEBS Lett **480**(2-3): 184-8.
Gomez-Puertas, P., J. Martin-Benito, et al. (2004). "The substrate recognition mechanisms in chaperonins." J Mol Recognit **17**(2): 85-94.
Grantham, J., O. Llorca, et al. (2000). "Partial occlusion of both cavities of the eukaryotic chaperonin with antibody has no effect upon the rates of beta-actin or alpha-tubulin folding." J Biol Chem **275**(7): 4587-91.
Guex, N. and M. C. Peitsch (1997). "SWISS-MODEL and the Swiss-PdbViewer: an environment for comparative protein modeling." Electrophoresis **18**(15): 2714-23.
Gutsche, I., L. O. Essen, et al. (1999). "Group II chaperonins: new TRiC(k)s and turns of a protein folding machine." J Mol Biol **293**(2): 295-312.
Hawes, B. E., K. Touhara, et al. (1994). "Determination of the Gßg-binding domain of phosducin. A regulatable modulator of Gßg signaling." Journal of Biological Chemistry **269**: 29825-29830.
Heymann, J. B. (2001). "Bsoft: image and molecular processing in electron microscopy." J Struct Biol **133**(2-3): 156-69.
Ho, Y., A. Gruhler, et al. (2002). "Systematic identification of protein complexes in Saccharomyces cerevisiae by mass spectrometry." Nature **415**(6868): 180-3.
Holm, L. and C. Sander (1993). "Protein structure comparison by alignment of distance matrices." J Mol Biol **233**(1): 123-38.
Humrich, J., C. Bermel, et al. (2005). "Phosducin-like protein regulates G-protein betagamma folding by interaction with tailless complex polypeptide-1alpha: dephosphorylation or splicing of PhLP turns the switch toward regulation of Gbetagamma folding." J Biol Chem **280**(20): 20042-50.
Humrich, J., C. Bermel, et al. (2003). "Regulation of phosducin-like protein by casein kinase 2 and N-terminal splicing." J Biol Chem **278**(7): 4474-81.
Jones, T. A., J. Y. Zou, et al. (1991). "Improved methods for building protein models in electron density maps and the location of errors in these models." Acta Crystallogr A **47 (Pt 2)**: 110-9.
Kasahara, S., P. Wang, et al. (2000). "Identification of bdm-1, a gene involved in G protein beta-subunit function and alpha-subunit accumulation." Proc Natl Acad Sci U S A **97**(1): 412-7.
Lacefield, S. and F. Solomon (2003). "A novel step in beta-tubulin folding is important for heterodimer formation in Saccharomyces cerevisiae " Genetics **165**: 531-541.

Lee, R. H., T. D. Ting, et al. (1992). "Regulation of retinal cGMP cascade by phosducin in bovine rod photoreceptor cells. Interaction of phosducin and transducin." Journal of Biological Chemistry **267**: 25104-25112.

Liou, A. K. and K. R. Willison (1997). "Elucidation of the subunit orientation in CCT (chaperonin containing TCP1) from the subunit composition of CCT micro-complexes." Embo J **16**(14): 4311-6.

Litchfield, D. W. (2003). "Protein kinase CK2: structure, regulation and role in cellular decisions of life and death." Biochem J **369**(Pt 1): 1-15.

Llorca, O., J. Martín-Benito, et al. (2000). "Eukaryotic chaperonin CCT stabilizes actin and tubulin folding intermediates in open quasi-native conformations." Embo J **19**: 5971-5979.

Llorca, O., E. A. McCormack, et al. (1999). "Eukaryotic type II chaperonin CCT interacts with actin through specific subunits." Nature **402**(6762): 693-6.

Loew, A., Y. K. Ho, et al. (1998). "Phosducin induces a structural change in transducin βγ." Structure **6**: 1007-1019.

Lukov, G. L., C. M. Baker, et al. (2006). "Mechanism of assembly of G protein betagamma subunits by protein kinase CK2-phosphorylated phosducin-like protein and the cytosolic chaperonin complex." J Biol Chem **281**(31): 22261-74.

Lukov, G. L., T. Hu, et al. (2005). "Phosducin-like protein acts as a molecular chaperone for G protein betagamma dimer assembly." Embo J **24**(11): 1965-75.

Lukov, G. L., C. S. Myung, et al. (2004). "Role of the isoprenyl pocket of the G protein beta gamma subunit complex in the binding of phosducin and phosducin-like protein." Biochemistry **43**(19): 5651-60.

Martin-Benito, J., S. Bertrand, et al. (2004). "Structure of the complex between the cytosolic chaperonin CCT and phosducin-like protein." Proc Natl Acad Sci U S A **101**: 17410-17415.

Martin-Benito, J., J. Boskovic, et al. (2002). "Structure of eukaryotic prefoldin and of its complexes with unfolded actin and the cytosolic chaperonin CCT." Embo J **21**(23): 6377-86.

Martin, J. L. (1995). "Thioredoxin--a fold for all reasons." Structure **3**(3): 245-50.

McLaughlin, J. N., C. D. Thulin, et al. (2002). "Regulatory interaction of phosducin-like protein with the cytosolic chaperonin complex." Proc. Natl. Acad. Sci. U. S. A. **99**(12): 7962-7967.

McLaughlin, J. N., C. D. Thulin, et al. (2002). "Regulation of angiotensin II-induced G protein signaling by phosducin-like protein." J Biol Chem **277**(38): 34885-95.

Meggio, F. and L. A. Pinna (2003). "One-thousand-and-one substrates of protein kinase CK2?" Faseb J **17**(3): 349-68.

Michaelson, D., I. Ahearn, et al. (2002). "Membrane trafficking of heterotrimeric G proteins via the endoplasmic reticulum and Golgi." Mol Biol Cell **13**(9): 3294-302.

Miles, M. F., S. Barhite, et al. (1993). "Phosducin-like protein: an ethanol-responsive potential modulator of guanine nucleotide-binding protein function." Proc Natl Acad Sci U S A **90**(22): 10831-5.

Pappenberger, G., J. A. Wilsher, et al. (2002). "Crystal structure of the CCTgamma apical domain: implications for substrate binding to the eukaryotic cytosolic chaperonin." J Mol Biol **318**(5): 1367-79.

Regelmann, J., T. Schule, et al. (2003). "Catabolite degradation of fructose-1,6-bisphosphatase in the yeast Saccharomyces cerevisiae: a genome-wide screen identifies eight novel GID genes and indicates the existence of two degradation pathways." Mol Biol Cell **14**(4): 1652-63.

Rockman, H. A., W. J. Koch, et al. (2002). "Seven-transmembrane-spanning receptors and heart function." Nature **415**(6868): 206-12.

Savage, J. R., J. N. McLaughlin, et al. (2000). "Functional roles of the two domains of phosducin and phosducin-like protein." J Biol Chem **275**(39): 30399-407.

Schoneberg, T., A. Schulz, et al. (2004). "Mutant G-protein-coupled receptors as a cause of human diseases." Pharmacol Ther **104**(3): 173-206.

Schroder, S. and M. J. Lohse (1996). "Inhibition of G-protein betagamma-subunit functions by phosducin-like protein." Proc Natl Acad Sci U S A **93**(5): 2100-4.

Schroder, S. and M. J. Lohse (2000). "Quantification of the tissue levels and function of the G-protein regulator phosducin-like protein (PhLP)." Naunyn Schmiedebergs Arch Pharmacol. **362**: 435-439.

Shevchenko, A., M. Wilm, et al. (1996). "Mass spectrometric sequencing of proteins silver-stained polyacrylamide gels." Anal Chem **68**(5): 850-8.

Siegers, K., B. Bölter, et al. (2003). "Tri-CCT cooperates with different upstream chaperones in the folding of distinct protein classes. ." Embo J **22**: 5230-5240.

Simonds, W. F. (2003). "G protein-regulated signaling dysfunction in human disease." J Investig Med **51**(4): 194-214.

Sokolov, M., K. J. Strissel, et al. (2004). "Phosducin facilitates light-driven transducin translocation in rod photoreceptors. Evidence from the phosducin knockout mouse." J Biol Chem **279**(18): 19149-56.

Thibault, C., M. W. Sganga, et al. (1997). "Interaction of phosducin-like protein with G protein betagamma subunits." J Biol Chem **272**(19): 12253-6.

Thulin, C. D., K. Howes, et al. (1999). "The immunolocalization and divergent roles of phosducin and phosducin-like protein in the retina." Mol Vis **5**: 40.

Valpuesta, J. M., J. Martín-Benito, et al. (2002). "Structure and function of a protein folding machine: the eukaryotic cytosolic chaperonin " FEBS Lett **529**: 11-16.

Valpuesta, J.M., Carrascosa, J.L. & Willison, K.R. (2004) in *Handbook of Protein Folding,* eds. Buchner, J. & Kiefhaber, T. (Wiley, New York), in press.

Wells, C. A., J. Dingus, et al. (2006). "Role of the chaperonin CCT/TRiC complex in G protein betagamma-dimer assembly." J Biol Chem **281**(29): 20221-32.

Willison, K.R., (1999) in *Molecular Chaperones and Folding Catalysts,* ed. Bukau, B. (Harwood Academic, Amsterdam), pp. 555–571.

Yoshida, T., B. M. Willardson, et al. (1994). "The phosphorylation state of phosducin determines its ability to block transducin subunit interactions and inhibit transducin binding to activated rhodopsin." J Biol Chem **269**(39): 24050-7.